UVB Damage and Photoreactivation in the Two-spotted Spider Mite, *Tetranychus urticae*

Yasumasa MURATA

Laboratory of Ecological Information,

Graduate School of Agriculture, Kyoto University

2017

CONTENTS

Chapter1: General Introduction

Solar radiation truistically plays essential role in natural ecosystem. The primary producer converts solar energy into chemical energy at the bottom of trophic level. Thus, sunlight can be the original source of life. Other hand, it is understandable that its staunch intense energy has various effects not only positively but also negatively for organisms. As one of the negative effects of solar radiation, there is the ultraviolet radiation, the shorter wavelength of sunlight.

Ambient ultraviolet radiation (UVR) causes deleterious effects in organisms through the induction of cytotoxic DNA lesions (Sinha and Häder 2002) and the production of reactive oxygen species (Jurkiewicz and Buettner 1994). Recently, more attention is paid for those effects because of attenuation of stratospheric ozone layer (United Nations Environment Programme, Environmental Effects Assessment Panel 2012). Particularly in the south Argentine (Tierra del Fuego), direct and indirect effects of UVR on biological interaction have been well studied since 1990s (Rousseaux et al. 2004; Caldwell et al. 2007; Ballaré et al. 2011). Furthermore, recent studies focus on the relations with climate changes and biological adaptations (Rozema et al. 2002; Bancroft et al. 2007; Foggo et al. 2007).

Solar UVR is divided into UVC (200–280 nm), UVB (280–315 nm), and UVA (315–400 nm). Since UVC is absorbed by oxygen and ozone, no UVC reaches the ground. Major part of UVB is also absorbed by ozone layer, and the small part reaches the ground with UVA. As a result, solar UVR spectrum consists of a major UVA and a minor UVB component. Shorter wavelengths are ordinary more deleterious to organisms. Consequently, in solar UVR wavelengths around 300 nm exert the strongest biological impact on organisms on the ground (Coohill and Sagripanti 2009).

Terrestrial animals are generally thought to be well protected from UV damage by their exoskeletons, coats or plumage, and/or effective mechanisms for repairs of UV damage (Paul and Gwynn-Jones 2003). However, recent studies demonstrated the vulnerability of plant-dwelling mites to solar and artificial UV radiation; e.g., irradiation with UVB causes lethal damage to two-spotted spider mite, *Tetranychus urticae* Koch (Ohtsuka and Osakabe 2009; Suzuki et al. 2009). Sakai et al. (2012) found that the hatchability of *T. urticae* eggs was negatively correlated with cumulative solar UVB irradiance but not with UVB intensity. Although intense UVB radiation in summer was expected to exert the greatest effect on survival of *T. urticae* (e.g., Barcelo 1981), egg hatchability was lowest in April (11%) and increased almost linearly until October (92%; Sakai et al. 2012).

Chapter 1

The Bunsen–Roscoe reciprocity law (hereafter, the reciprocity law) states that as long as the product of irradiance and the time of exposure is the same the photochemical effect will be the same (Dworkin 1958); i.e., the extent of photochemical effects is determined by cumulative irradiance (J m^{-2}) [= irradiance (W m^{-2}) × irradiation period (s)]. The reciprocity law might also be applicable to UV damage in organisms, e.g., the amount of DNA lesions in an aquatic arthropod, *Daphnia* sp. (Connelly et al. 2009), and the extent of disinfection of the airborne bacterium *Serratia marcescens* (Riley and Kaufman 1972). Reciprocity in survivorship under UVB radiation has also been demonstrated in shrimp zoea (Wübben 2000), early life stages of sea urchin (Nahon et al. 2009) and fish eggs (Kouwenberg et al. 1999b). However, mortality of shrimp zoea after UVB irradiation at low intensity (0.2 W m^{-2}) diverged from the reciprocity law, which had been upheld under radiation at higher irradiances (Wübben 2000). Similar divergence from reciprocity in UVB damage was also found for several cases of aquatic animals (Cywinska et al. 2000). Therefore, there are some inapplicabilities of the reciprocity law to UV damage.

The UVB effect on terrestrial organisms has not been well studied, thus far there is little information including the application of reciprocity law. Most previous studies have been conducted using aquatic animals. The verification about UVB effect using terrestrial organisms could be the first to beginning of ecological and physiological evaluation for terrestrial adaptation to solar UV.

One of the most important targets of UVB harmful effects is DNA (Peak et al. 1984; Sinha and Häder 2002). UVB radiation causes DNA damage in organisms, including the formation of pyrimidine dimers such as cyclobutane pyrimidine dimers (CPD) and pyrimidine (6-4) pyrimidone photoproducts (Sinha and Häder 2002). Two major DNA repair mechanisms: excision repair (dark repair pathways: base excision repair and nucleotide excision repair) and photo-enzymatic repair (PER) on UV-induced DNA damage have been being studied recently (Malloy et al. 1997). Excision repair is a multiple enzyme system that replaces the damaged DNA with new, undamaged nucleotides using energy derived from ATP (Sinha and Häder 2002). In PER, DNA lesions are directly repaired by a photolyase using energy from blue visible light (400–450 nm wavelength; Sancar 2003) and ultraviolet-A (UVA; 315–400 nm wavelength; Kelner 1949; Kalthoff 1975; Shiroya et al. 1984; Sinha and Häder 2002). Excision repair is found in all taxa but is not specific repair mechanism of UV-induced DNA damage. In contrast, PER is specific for UV-induced DNA damage but is not present in all taxa (Sancar 1994b). The enzyme involved in PER, photolyases, are categorized into CPD photolyase and (6-4) photolyase, which specifically bind to CPDs and 6-4PPs,

respectively. However, the distribution of each photolyase lacks coherence among organisms. (6-4) photolyase PER function is absent in placental mammals (Sinha and Häder 2002; Karentz 2015). In fact, humans do not possess photolyase (Li et al. 1993; Thoma 1999; Sancar 2003).

As well as UVB effects, photoreactivation and its proximate mechanism hardly studied in terrestrial organisms. Particularly, in Acari, Santos (2005) reported photoreactivation in adult females (survival recovery) of *T. urticae* and the mold mite, *Tyrophagus putrescentiae* (Schrank), caused by irradiation by flood lamp after exposure to UVB radiation. Recent genomics revealed presence of four CPD photolyase genes in *T. urticae* genome (Grbić et al. 2011). However, more detail demonstrations have never been conducted.

In this study, I verified the UVB-induced biological impact and photoreactivation effect on *T. urticae*. To best of my knowledge, this will be the first assessment on terrestrial animals.

In the terrestrial ecosystems, organisms are potentially exposable to direct solar UVR and thus the biological impact might be larger than aquatic ecosystems with surrounding water. From the broad perspective of the evolution, it is reasonable to suppose that the adaptation to solar UVR is one of the essential keys to advance from sea into terrestrial world for organisms when much more intense UVB reached the ground in ancient times. Detailed information about UVB damage and photoreactivation effect on *T. urticae* fitness could lead better understanding of the adaptation to solar radiation and enable to evaluate its significance for the biological evolution. Recent study revealed that the main predators of spider mite, phytoseiid mites (Acari: Phytoseiidae) were also vulnerable to UVB (Tachi and Osakabe 2012, 2014). By integrating such information, the novel ecological insight will potentially be shed on the interaction among herbivores, carnivores, and plants via sun light.

UVB-induced DNA damage and its repair have thought to be deeply related to survivals (Malloy et al. 1997; Sinha and Häder 2002; Connelly et al. 2009). However, physiological studies about UV effect have hardly been conducted using terrestrial animals. Particularly, terrestrial arthropods have never been focused as the research material. If UVB-induced DNA damage is proved on *T. urticae*, it will become the important evidence of physiological impact of UV on terrestrial ecosystem. In addition, the same situation is true of photoreactivation mechanism. The main mechanism of photoreactivation has been thought to be repairing such DNA damages by photolyase function (Sancar 2003), but whether there is the same function also in terrestrial living arthropods, has never been verified. Demonstration of photoreactivation mechanism of

T. urticae will indicate the existence and importance of that function for physiological adaptation to UVB. Furthermore, these can become base knowledge to explore details and validate various possibilities about physiological mechanism of UVB damage and its repair.

Spider mites including *T. urticae* are ubiquitous polyphagous arthropods which can feed on pretty board range of plant species and thus an economically important agricultural pest worldwide. For management of this pest, the chemical control using acaricides have been conducted for long time. However, because of their high fecundity and short life cycle, the acaricide-resistant phenotype easily becomes dominant in population. The alternative strategy to chemical control has been strongly required. Ohtsuka and Osakabe (2009) first reported the lethal effect induced by UVR on *T. urticae*. Recently, companies and research institutions have attempted to apply this UV lethal effect to pest management as physical strategy. Particularly, in Japan, some exploratory programs for mite management in greenhouses using artificial UVB lamps are already being performed (Masui et al. 2013; Tanaka et al. 2016). Under these circumstances, understanding how UVB affect *T. uritcae* and elucidating its physiological mechanisms should contribute to developing this new mite management system.

Moreover, it would say that *T. urticae* is a suitable organism to study UVB damage and photoreactivation repair here for following four reasons: (1) their population may easily increase, which is one of the reasons for their being an important pest; (2) their vulnerability to UVB was well known by recent studies (Ohtsuka and Osakabe 2009; Suzuki et al. 2009; Onzo et al. 2010; Sakai and Osakabe 2010; Sakai et al. 2012; Fukaya et al. 2013); (3) many behavioral traits affected by UV were reported (Barcelo and Calkins 1980; Barcelo 1981; Sakai and Osakabe 2010); (4) their genome data have already been available (Grbić et al. 2011).

The primary objective of this study is to quantify *T. urticae*'s vulnerability to UVB and photoreactivation capacity. First, I elucidated whether the reciprocity law is applicable to UVB damage of *T. urticae* (Chapter3). I examined egg hatchability and survival of larvae, teleiochrysalises and adult females after irradiation with UVB at various combinations of intensity and time lengths using a UVB lamp. Effects on egg production and developmental rate were also evaluated. Second, I assessed the photoreactivation capacity of *T. urticae* by testing whether visible light irradiation by halogen lamp (VIS) increased survivorship after exposure to UVB radiation (Chapter4). I evaluated the efficacy of photoreactivation and the factors affecting photoreactivation in *T. urticae*. The effects of the time lag between UVB and VIS irradiation and

wavelengths of light (including VIS and UVA) on photoreactivation were also tested. Third, I quantified CPDs and 6-4PPs induced by UVB irradiation and evaluated the reduction of DNA lesions by PER and NER under light and dark conditions, respectively, in *T. urticae*. To evaluate the role of each enzymatic repair, I analysed the interaction between the DNA lesion amount and the gene expression levels of repair enzymes, CPD photolyase for PER and xeroderma pigmentosum group A (XPA) protein for NER, associated with UVB and VIS irradiation (Chapter 5). At last, I conducted the observation of larvae exposed to high lethal level of UVB and demonstrated the protochrysalis phase-specific death (Chapter 6). Actually, in the case of larvae, the individuals exposed to UVB radiation seemed phenotypically normal. However, when they developed to the next protochrysalis stage, UVB-induced death was severely occurred. Many individuals fault moulting being trapped in old epidermis, or stop development and shrink. The chrysalis stage is assumed dynamic physiological changes about body formation of next developmental stage and to be deeply related to UVB-induced mortality. In order to explore the causes of such specific death, the whole transcriptomes were profiled between protochrysalis individuals which were exposed/non-exposed to UVB radiation when they were at larval stages to clarify the differentially expressed genes and find a clue of mechanism elucidation causing phase-specific mortality.

Chapter2: Materials, Equipment, and Laboratory Conditions

Mites

T. urticae is a significantly polyphagous cosmopolitan spider mite and thus an economically important agricultural pest. The mite population used in this study was established from several areas in Japan and was reared on kidney bean plant leaves in a chamber at 25°C under a 16-h light: 8-h dark (16 L:8 D) photoperiod for more than 1 year.

UVB lamp used in the investigation of UVB-induced mortality and phase-specific lethal effect (Chapter3, 6)

UVB irradiation was performed at 25°C in the laboratory, whose interior was illuminated by fluorescent lamps. Eggs or mites on leaf disks in Petri dishes were placed on four shelves located at different distances (0.45, 0.85, 1.35, and 1.75 m) from an overhead UVB lamp (YGRFX21701GH; Panasonic Co., Osaka, Japan) affixed at the top of a steel rack (1.9 m high × 0.6 m width × 0.6 m depth). The intensities of UVB (280–320 nm) received by the Petri dishes on the shelves were 0.19 (UVA+UVB: 0.27), 0.31 (0.45), 0.58 (1.0), and 1.55 (2.8) W m^{-2}, respectively ($X1_1$ Optomerter; Gigahertz-Optik Inc., Newburyport, MA). The highest solar UVB irradiances at ground level in Japanese main islands over seasons are around 2 W m^{-2} (Nozawa et al. 2007, 2010). The UVB irradiances used in this study was thus within the ambient solar UVB radiation in Japan. The frame of the shelves (steel rack) was covered with UV-opaque film (0.1 mm thick polyvinyl chloride film, Cutaceclean Kirinain; MKV Platech Co. Ltd., Tokyo, Japan) that filtered out UV. Petri dishes assigned as controls were placed on an adjoining shelf outside of the UV opaque film (UVB irradiance = 0 W m^{-2}).

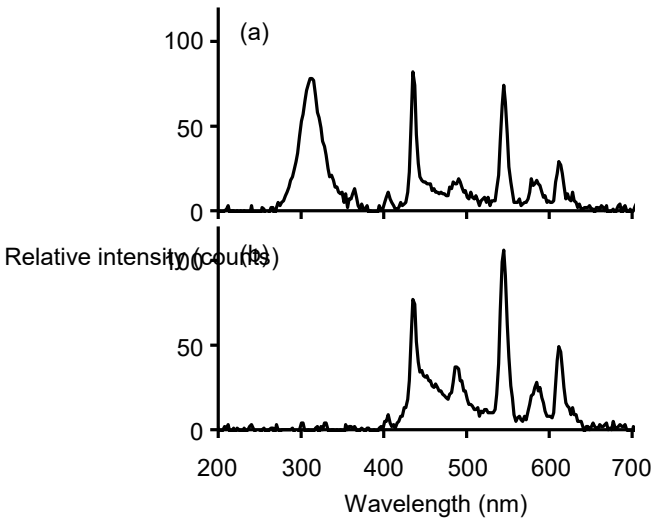

Fig. 1. Wavelength spectrums observed on experimental shelves under UVB irradiances of 0.31 (UVA+UVB: 0.45) W m^{-2} (a), and 0 W m^{-2} (outside of the shelf frame) (b).

The output of the UV lamp peaked at a wavelength of 310 nm. The spectrum of relative intensity was measured using a spectrometer (UFV-VIS F; Spectra Co-op Co., Tokyo, Japan; Fig. 1). Except for period of UVB irradiation, the Petri dishes were kept in the laboratory at 25°C and 16:8 h L:D light cycles (fluorescent lights were turned on at 07:00 h and off at 23:00 h).

UVB lamp and halogen lamps for visible light irradiation used in the investigations of photoreactivation phenomenon, UVB-induced DNA damage detection, and photo-enzymatic repair (Chapter4, 5)

A UVB lamp (6 W; Panasonic Electric Works Co. Ltd., Osaka, Japan) and two halogen lamps (130 W; JDR110V-85WHM/K7-H; Ushio Lighting Co. Ltd., Tokyo, Japan; set at an interval of 22.5 cm) were affixed from a shelf 67 cm overhead in a dark growth chamber at 25°C. The irradiance values of the UVB lamp and halogen lamps (VIS) on the shelf were 0.16 and 67.7 W m^{-2}, respectively. The UVB radiation peaked at 310 nm (Fig. 2a). The halogen lamp radiation included a small UVA fraction (Fig. 2b). The effects of wavelengths of light on photoreactivation were tested using each filtered-VIS (Fig. 2c) and UVA lamp (Fig. 2d). The UVB irradiance was measured using an irradiance meter ($X1_1$) equipped with a UV-3702-4 detector head (Gigahertz-Optik GmbH, Türkenfeld, Germany). The VIS irradiance was measured using a photo-radiometer (HD2102.2) equipped with an irradiance measurement probe (LP 471 RAD; Delta OHM, Padova, Italy). The wavelength spectra (indexed by relative intensity [counts]) were measured for each experimental setup using a spectrometer (UFV-VIS F; Spectra Co-op Co., Tokyo, Japan).

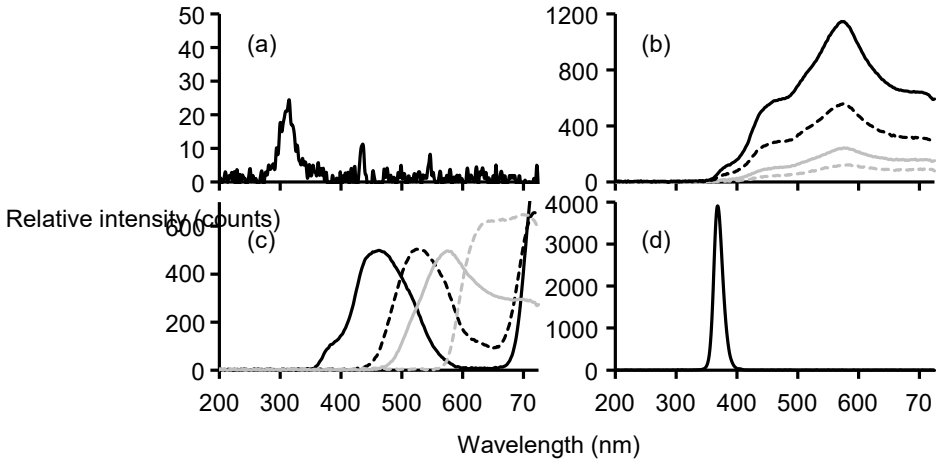

Fig. 2. Wavelength spectra of UVB, UVA, and VIS. (a) UVB lamp. (b) Halogen lamp (grey dashed line, 21.6 W m^{-2}; grey line, 36.8 W m^{-2}; dashed line, 67.7 W m^{-2}; solid line, 142 W m^{-2}). (c) Wavelength-filtered VIS (solid line, blue; dashed line, green; grey line, yellow; grey dashed line, red). (d) UVA lamp.

Chapter3: UVB-induced Damage of the Two-spotted Spider Mite *Tetranychus urticae*

Ambient ultraviolet (UV) radiation causes deleterious effects in organisms through the induction of cytotoxic DNA lesions (Sinha and Häder 2002), and the production of reactive oxygen species (Jurkiewicz and Buettner 1994). Recent literature has documented the harmfulness of solar and artificial UV radiation to plant-dwelling mites, such as the herbivorous two-spotted spider mite *Tetranychus urticae* Koch (Ohtsuka and Osakabe 2009; Suzuki et al. 2009), as well as predaceous phytoseiid mites (Ohtsuka and Osakabe 2009; Onzo et al. 2010; Tachi and Osakabe 2012). Of the range of UV wavelengths, damage to *T. urticae* is induced by ultraviolet-B (UVB, 280–315 nm wavelengths; Sakai and Osakabe 2010). Sakai and Osakabe (2010) concluded that escape from UVB damage was the main factor determining the typical location of *T. urticae* on the lower leaf surfaces of host plants.

The reciprocity law states that as long as the product of irradiance and the time of exposure is the same the photochemical effect will be the same (Dworkin 1958); i.e., the extent of photochemical effects is determined by cumulative irradiance (J m^{-2}) [= irradiance (W m^{-2}) × irradiation period (s)]. The reciprocity law might also be applicable to UV damage in organisms, e.g., the amount of DNA lesions in an aquatic arthropod, *Daphnia* sp. (Connelly et al. 2009), and the extent of disinfection of the airborne bacterium *Serratia marcescens* (Riley and Kaufman 1972). Reciprocity in survivorship under UVB radiation has also been demonstrated in shrimp zoea (Wübben 2000), early life stages of sea urchin (Nahon et al. 2009) and fish eggs (Kouwenberg et al. 1999b). However, mortality of shrimp zoea after UVB irradiation at low intensity (0.2 W m^{-2}) diverged from the reciprocity law, which had been upheld under radiation at higher irradiances (Wübben 2000). Similar divergence from reciprocity in UVB damage was also found for several cases of aquatic animals (Cywinska et al. 2000). Therefore, applicability of the reciprocity law to UV damage in organisms is still disputable.

Sakai et al. (2012) found that the hatchability of *T. urticae* eggs experimentally exposed to solar UVB radiation was negatively correlated with cumulative UVB irradiance but not with UVB intensity. Although intense UVB radiation in summer was expected to exert the greatest effect on survival of *T. urticae* (e.g., Barcelo 1981), egg hatchability was lowest in April (11%) and increased almost linearly until October (92%; Sakai et al. 2012).

In this chapter, I aimed to elucidate whether the reciprocity law is applicable to UVB

damage of *T. urticae*. I examined egg hatchability and survival of larvae, teleiochrysalises, and adults after irradiation with UVB at various combinations of intensity and time lengths using a UVB lamp. Effects on egg production and developmental rate were also evaluated.

Section1: Reciprocity Law in UVB Induced Mortality

- Materials and methods

Effects on egg hatchability

I prepared eight Petri dishes (9 cm in diameter). Four kidney bean leaf disks (2 × 2 cm) were placed on water-soaked cotton in each of the Petri dishes. Five adult *T. urticae* females were introduced onto each leaf disk. These Petri dishes were placed in the laboratory (25°C, 16:8 h L:D). After 24 h, the adult females were removed, and eggs laid on the leaf disks were counted. Two Petri dishes were then placed on each of three shelves for irradiation at 0.19, 0.31, and 0.58 W m^{-2} of UVB radiation, and the remaining two dishes were placed on the adjoining shelf as controls (0 W m^{-2}). I immediately exposed these eggs to UVB radiation for 15, 30, 60, or 90 min. Using the same procedure, eggs were also exposed to treatments irradiated with 0 (control), 0.31, and 0.58 W m^{-2} UVB for 10 min, and with 0, 0.19, and 0.31 W m^{-2} for 120 min.

A series of treatments was performed once. The numbers of eggs used for each combination of UVB intensity and irradiation time length (two Petri dishes containing eight leaf disks) were 283–453 in total (20–63 eggs per leaf disk except one leaf disk assigned for 0 W m^{-2} for 10 min exposure, on which only three eggs were available because four adult females had escaped from a leaf disk during the oviposition period).

After exposure to UVB radiation, the Petri dishes were returned to the laboratory where they had been reared before treatment (25°C, 16:8 h L:D). Hatchability was checked on day 6 after exposure, as I had previously confirmed that few eggs hatched after 6 days postexposure.

Effects on larvae

Two kidney bean leaf disks (2 × 2 cm) were placed on water-soaked cotton in each of four Petri dishes for each batch. Five adult *T. urticae* females were introduced onto each leaf disk in the laboratory (25°C, 16:8 h L:D). After 24 h, adult females were removed. Two days later (day 2 after the removal of adult females), I checked egg status and

removed hatched larvae if present. On day 3, I counted the number of larvae hatched within 24 h and removed unhatched eggs. One Petri dish (two leaf disks) was placed on each of three shelves, 0.19, 0.31, and 0.58 W m^{-2}, and on the adjoining shelf as a control (0 W m^{-2}). I then exposed these larvae to UVB radiation for 30, 45, or 60 min. Using the same procedure, larvae were also irradiated using treatments with 0 (control) and 0.58 W m^{-2} for 15 min; 0 and 0.31 W m^{-2} for 90 min; 0, 0.19, and 0.31 W m^{-2} for 120 min; and with 0 and 0.19 W m^{-2} for 180 min.

A series of treatments was performed twice. The numbers of larvae used for each combination of UVB intensity and irradiation time length (two Petri dishes containing four leaf disks) were 49–95 in total (21–48 larvae per treatment).

After exposure to UVB irradiation, larvae were individually transferred to newly prepared leaf disks (1.5 × 1.5 cm) on water-soaked cotton in Petri dishes in the laboratory (25°C, 16:8 h L:D). I then checked the survival rate, developmental stage, and sex of individuals that attained maturity every day until all individuals had developed to adulthood or died (day 9). Individuals remaining at a particular chrysalis stage for more than 5 days were judged to be dead.

Effects on teleiochrysalis females

One kidney bean leaf disk (4 × 4 cm) was placed on water-soaked cotton in each of four Petri dishes. From 30 to 32 teleiochrysalis females (quiescent stage of deutonymph just before the last molt to adulthood) were introduced onto each leaf disk. One Petri dish was placed on each of three shelves, 0.19, 0.31, and 0.58 W m^{-2}, and on the adjoining shelf as a control (0 W m^{-2}). I exposed these teleiochrysalis females to UVB radiation for 60, 120, or 180 min. Using the same procedure, teleiochrysalis females were also irradiated using treatments with 0 (control), 0.58, and 1.55 W m^{-2} for 30 min, and with 0 (control), 0.19, and 0.31 W m^{-2} for 240 min.

A series of treatments was performed once. The numbers of teleiochrysalis females used for each combination of UVB intensity and irradiation time length (one leaf disk) were 29–32.

After exposure to UVB radiation, I removed individuals that had moulted during exposure to UVB radiation. These females were reared in the laboratory (25°C, 16:8 h L:D). The proportion of moulting individuals was checked 3 days after exposure because I preliminary confirmed that few individuals molted after 3 days post-exposure.

Effects on adult females

One kidney bean leaf disk (4 × 4 cm) was placed on water-soaked cotton in each of

four Petri dishes. Twenty teleiochrysalis females were introduced onto each leaf disk. To raise the relative humidity (RH) on the leaves, the Petri dishes were covered with transparent plastic lids. Under humid conditions, tetranychid mites in the quiescent stage delay moulting (Ikegami et al. 2000). After 2 days (day 0), the lids were removed and most adult virgin females emerged within 30 min. Three days later (day 3), I counted newly emerged adult females. One Petri dish was placed on each of three shelves, 0.31, 0.58, and 1.55 W m^{-2}, and on the adjoining shelf as a control (0 W m^{-2}). I exposed these adult females to UVB radiation for 6 h. Using the same procedure, adult females were also irradiated using treatments with 0 (control), and 1.55 W m^{-2} for 2 and 10 h, and with 0, 0.31, and 0.58 W m^{-2} for 14 and 24 h.

A series of treatments was performed three times. The numbers of adult females for each combination of UVB intensity and irradiation time length (three Petri dishes containing three leaf disks) were 41–60 in total; 13–20 females per treatment except two leaf disks assigned for 0 W m^{-2} for 14 h and 24 h exposure, on which 4 and 9 adult females, respectively, were available because of excessive failure to moult.

After exposure to UVB radiation, adult females were individually transferred to newly prepared leaf disks (1.5 × 1.5 cm) on water-soaked cotton in Petri dishes in the laboratory (25°C, 16:8 h L:D). I checked the survival rates after 3 days (day 6) because I preliminary confirmed that individuals died due to UVB damage were clearly distinctive from living mites. Females escaped from leaf disks were included in the number of dead individuals. The number of eggs laid on each leaf disk was also checked on day 3.

Data analysis

Mortality in each treatment was corrected following Abbott's formula (1) (Abbott 1925),

$$M = \frac{1 - X}{Y - X} \times 100 \quad (1),$$

where M, X, and Y represent the %-corrected mortality, the natural (control) death rate of eggs, and the death rate of individuals (eggs) exposed to UVB radiation, respectively, in each treatment. For this calculation, the number of individuals (eggs) on leaf disks was pooled in each treatment (no replication experiment).

The corrected mortalities were transformed to probits except for data on 0 or 100% mortality. To evaluate the effects of UVB intensity on mortality, the data set for each developmental stage was used in an analysis of covariance (ANCOVA) using R software ver. 2.14.0 following Aoki (2011). In ANCOVA, the cumulative UVB

irradiances, mortality probits and UVB intensities were used as independent variables, dependent variables, and group variables, respectively. If no significant differences were detected in slopes and mean mortalities among different intensities, linear regression analysis was applied to the data set using the "lm" module of R. LD_{50} values and associated standard errors were obtained using the "dose.p" module in the package MASS, and 95% confidence intervals of the LD_{50} values were calculated based on the 97.5% point of cumulative probability distribution in the t-distribution predicted using the "qt" module of R.

The effects of UVB intensity on the developmental rate were also evaluated by ANCOVA using R following Aoki (2011). In ANCOVA, the cumulative UVB irradiances, developmental days, and UVB intensities were used as independent variables, dependent variables, and group variables, respectively. If no significant differences were detected in slopes and mean mortalities among different intensities, linear regression analysis was applied to data sets with all UVB intensities combined, except controls (0 W m^{-2}), using the "lm" module of R.

For the analysis of egg production, linear regression analysis was applied to the data sets with all UVB intensities combined, except for females with no egg production, using the "lm" module of R. I did not apply ANCOVA because the sample sizes for individual intensities were too low.

- Results

Mortality regression on cumulative UVB irradiance and LD_{50}

Mortality increased with cumulative doses of irradiation, and no differences in mortality were observed among UVB intensities for eggs, larvae, and adult females (Fig. 3a, b, d, respectively). Larvae were not likely to be affected by UVB irradiation in terms of their behavior and activity after exposure to UVB radiation, and most entered the protochrysalis stage normally, even at the higher cumulative UVB irradiance. However, many individuals died during the protochrysalis stage or failed to moult to the protonymphal stage and died. In contrast, the mortality of teleiochrysalis females also increased with increasing cumulative UVB irradiance but reached a plateau at 2.8 kJ m^{-2} (Fig. 3c).

ANCOVA using probit mortalities revealed that neither the slope nor average mortality significantly differed among UVB intensities for all life stages (egg, slope: $F_{[2,8]} = 3.2492$, $P = 0.09270$, average: $F_{[2,10]} = 2.2925$, $P = 0.1515$; larva, slope: $F_{[2,4]} = 1.1567$, $P = 0.4014$, average: $F_{[2,6]} = 0.01909$, $P = 0.9811$; teleiochrysalis female, slope:

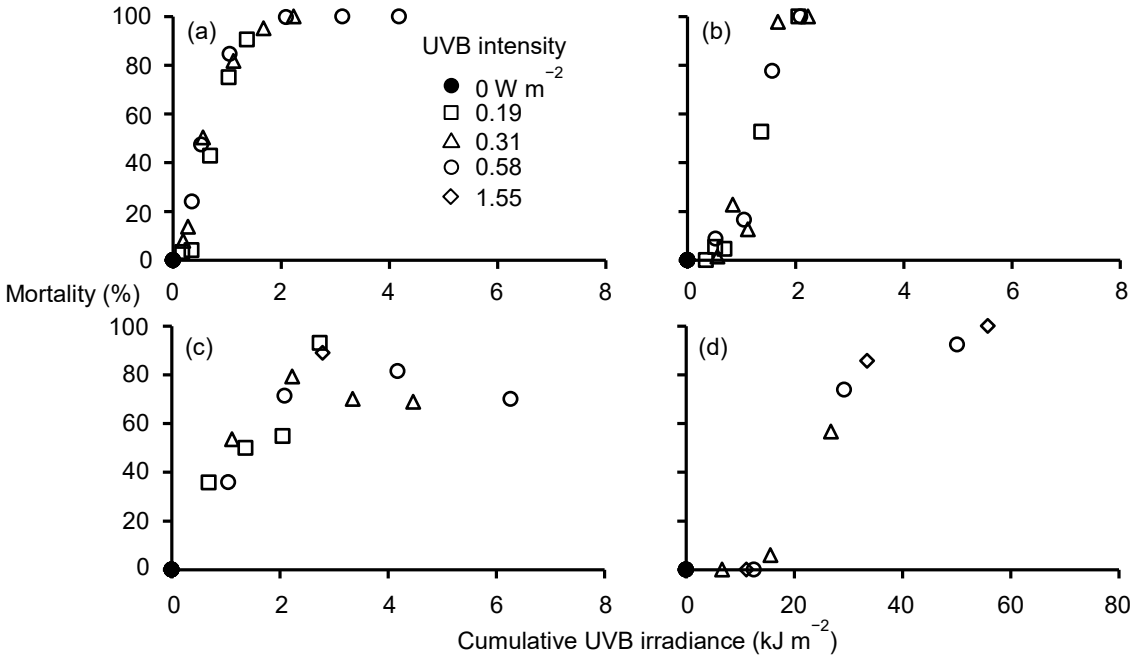

Fig. 3. Relationship between cumulative UVB irradiance and mortality of eggs (a), larvae (b), teleiochrysalis females (c), and adult females (d) after exposure to UVB radiation at different intensities and irradiation time length.

$F_{[2,6]}$ = 2.8399, P = 0.1356, average: $F_{[2,8]}$ = 0.1893, P = 0.8312), except for adult females, which were not analyzed using ANCOVA. I observed strong positive linear correlations between probit mortality and cumulative UVB irradiance for eggs, larvae, and adult females (Fig. 4). The LD_{50} value was highest in adult females, followed by larvae and eggs (Table 1). Although I detected a significant positive linear correlation for teleiochrysalis females, both the slope and coefficient of determination (R^2) were much smaller than those observed for the other developmental stages, causing the LD_{50} value to be equivalent to that in larvae (versus adult females; Fig. 4, Table 1).

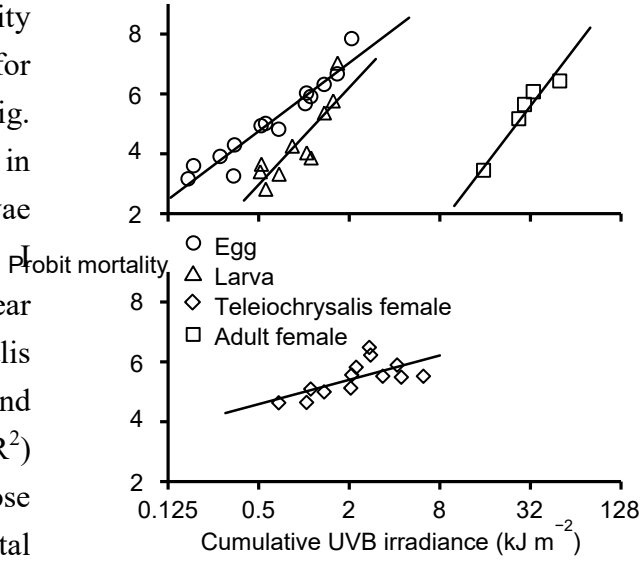

Fig. 4. Relationship between cumulative UVB irradiance and probit mortality of eggs, larvae, teleiochrysalis females, and adult females. Formulas and coefficients of determination (R^2) of the linear regression lines are shown in Table 1.

Table 1. Linear regression of probit mortality on cumulative UVB irradiance (kJ m^{-2}) and LD_{50} values in eggs, larvae, teleiochrysalis females, and adult females

Developmental stage	Regression formula[a]	R^2	P value	LD_{50} (kJ m^{-2})	95% confidence interval
Egg	$y = 1.6485\ln(x) + 5.8904$	0.9181	4.346×10^{-8}	0.58	0.51–0.67
Larva	$y = 2.3492\ln(x) + 4.5864$	0.7082	0.001392	1.19	0.94–1.52
Teleiochrysalis	$y = 0.5864\ln(x) + 4.9956$	0.3944	0.01277	1.01	0.48–2.10
Adult	$y = 2.866\ln(x) - 4.352$	0.8897	0.01036	26.12	21.64–31.52

Effects of UVB irradiation on larvae and subsequent developmental rates

In individuals that had developed from larvae to adulthood after exposure to UVB radiation at the larval stage, no differences were observed in the number of developmental days among UVB intensities for either females or males (ANCOVA: female, slope: $F_{[2, 3]} = 0.1275$, $P = 0.8848$, average: $F_{[2, 5]} = 2.7394$, $P = 0.1573$; male, slope: $F_{[2, 3]} = 0.2295$, $P = 0.8077$, average: $F_{[2, 5]} = 1.3624$, $P = 0.3371$; Fig. 5).

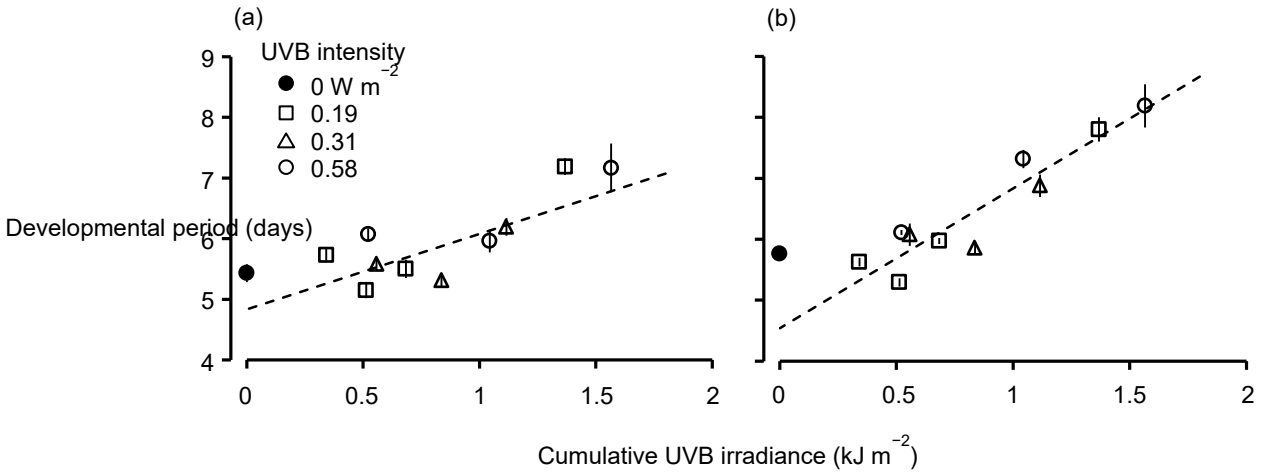

Fig. 5. Effects of cumulative UVB irradiance on developmental duration from larvae to adult emergence in males (a) and females (b). Vertical lines on plots represent standard errors. Broken lines in the figures show linear regression lines calculated using combined data sets over all UVB intensities, except controls (males: $y = 1.2454x + 4.8320$, $R^2 = 0.6292$, $P = 0.006564$; females: $y = 2.2946x + 4.5381$, $R^2 = 0.832$, $P = 0.0003769$).

Because only one female and one male developed to adulthood, data for UVB intensity at 0.31 W m^{-2} for 90 min (1.674 kJ m^{-2}) exposure were excluded from the data analysis. The developmental period was prolonged with increasing cumulative UVB irradiance. I observed a significant positive linear relationship between cumulative UVB irradiance and developmental period, except for the control (0 W m^{-2}), in both females and males

(males: $y = 1.2454x + 4.8320$, $R^2 = 0.6292$, $P = 0.006564$; females: $y = 2.2946x + 4.5381$, $R^2 = 0.832$, $P = 0.0003769$). However, the y-intercept (4.8 and 4.5 days in males and females, respectively) was obviously smaller than that for the developmental period of individuals in controls [0 W m^{-2}, 5.4 ± 0.1 (SE) and 5.8 ± 0.1 days in males and females, respectively; Fig. 5]. Using the linear regression, the cumulative UVB irradiance corresponding to the developmental periods in controls was back-calculated to be 0.48 and 0.53 kJ m^{-2} in males and females, respectively. Therefore, cumulative UVB irradiance below 0.5 kJ m^{-2} may have no to slight negative effects on the rate of subsequent juvenile development, regardless of the intensity of UVB radiation. Consequently, the reciprocity law was upheld in juvenile development when cumulative UVB irradiance exceeded 0.5 kJ m^{-2}. However, negative effects did not occur below 0.5 kJ m^{-2}.

Effects of UVB irradiation on adult females and subsequent egg production

In adult females, egg production was reduced with increasing cumulative UVB irradiance (Fig. 6). Females that survived after exposure to 0.58 W m^{-2} for 24 h (50.112 kJ m^{-2}) of UVB radiation (n = 4) and laid no eggs were excluded from Fig. 6 and the linear regression analysis. The number of eggs did not remarkably differ among UVB intensities at the corresponding cumulative irradiance. I detected a significant negative linear relationship between cumulative UVB irradiance and egg production using the combined data set ($y = -1.3282x + 44.8954$, $R^2 = 0.906$, $P = 0.0001686$; Fig. 6). Therefore, the reciprocity law was upheld for egg production.

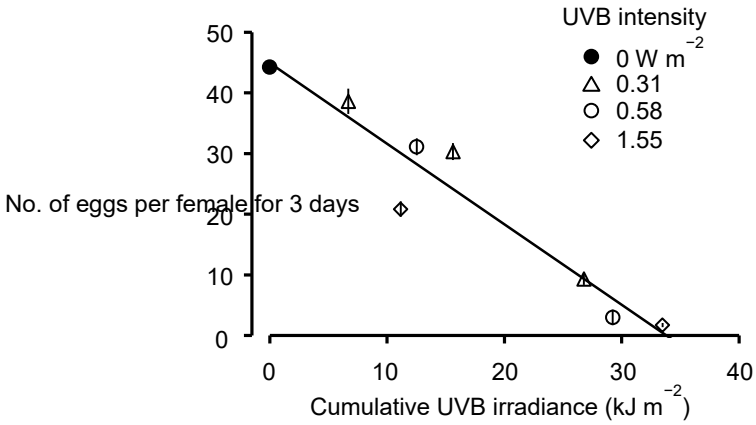

Fig. 6. Cumulative UVB irradiance and egg production by females that survived for 3 days after UVB treatment. Vertical lines on plots represent standard errors. The solid line shows the linear regression for the data set pooled over UVB intensities ($y = -1.3282x + 44.8954$, $R^2 = 0.906$, $P = 0.0001686$). Females surviving after exposure to 50.112 kJ m^{-2} UVB radiation (n = 4) that did not lay eggs were excluded from the figure and the linear regression analysis.

- Discussion

These results showing the reciprocity law are consistent with those of Sakai et al. (2012); the hatchability of *T. urticae* eggs experimentally exposed to solar UVB radiation was negatively correlated with cumulative UVB irradiance but not with UVB intensity.

Although the significant positive linear correlation was observed between cumulative UVB irradiance and probit mortality in *T. urticae* teleiochrysalis females, the R^2 value and slope of the regression line were small. In contrast, larvae exposed to UVB radiation died primarily during the protochrysalis stage or later when failing to molt to protonymphs. Moreover, the LD_{50} value was similar in *T. urticae* teleiochrysalis females (quiescent stage just before adults) to larvae despite a larger body size. These results suggest that the physiological mechanism for ecdysis was vulnerable to damage from UVB. Vulnerability during chrysalis stages may differ depending on the phase preceding moulting, which may be why the survivals of teleiochrysalis were diverse and more similar to that of larvae than of adult females, despite a larger body size as teleiochrysalises than as larvae.

In regard to solar radiation, daily cumulative UVB irradiance is highest in summer (generally July and August) and lowest in winter (December and January) in the midlatitudes of the Northern Hemisphere. According to the Solar Radiation and Weather Monitoring Project at Kyoto Women's University (http://www.cs.kyoto-wu.ac.jp/~konami/climate/index.shtml), maximum and minimum daily solar UVB irradiance were 21.8 and 4.3 kJ m^{-2}, respectively, in Kyoto, Japan (34°59'N, 135°47'E) during 2009–2010. Therefore, the maximum daily irradiance was close to the LD_{50} value of adult females, and even minimum daily irradiance exceeded the LD_{50} values of eggs, larvae, and teleiochrysalis females obtained in the laboratory. However, Sakai et al. (2012) estimated that the LD_{50} of *T. urticae* eggs caused by solar UVB radiation was about 50 kJ m^{-2}. This value is around 100 times the LD_{50} for eggs (0.58 kJ m^{-2}) and twice that for adult females (26.12 kJ m^{-2}) determined in our laboratory experiments using a UV lamp.

Such differences between damage by the UV lamp and solar UV radiation also likely occur for effects on the egg production of adult females. Sakai and Osakabe (2010) tested irradiation effects on egg production by exposing *T. urticae* adult females to solar UV radiation under UV-transparent and UV-opaque film. They observed a reduction in the egg production of females exposed to solar UV radiation (under UV transparent film; Sakai and Osakabe 2010). However, the reduction was less than 30% of that

observed for egg production by females under UV-opaque film, despite cumulative UVB radiation values for UV-transparent and UV-opaque film being 84.6 and 49.7 kJ m^{-2}, respectively. In this study, the cumulative UVB irradiance at which egg production is zero, as calculated from the regression line, is 33.8 kJ m^{-2}. In actuality, most adult female individuals died and the survivors laid no eggs after exposure to 50.112 kJ m^{-2} UVB radiation.

The potential mechanism causing such variation in LD_{50} values between laboratory and field studies may be the photoenzymatic repair of UVB-induced DNA damage (Kalthoff 1975; Sinha and Häder 2002; Macfadyen et al. 2004). In fact, Santos (2005) has suggested such a function of photoreactivation in *T. urticae* adult females. Moreover, recent coding sequence (CDS) analyses have revealed the presence of several cyclobutane pyrimidine dimer (CPD) photolyase genes in the *T. urticae* genome (Grbić et al. 2011). Photoenzymatic repair of DNA lesions with the aid of photolyase is one of the most important repair mechanisms that frequently occurs in many organisms (Sinha and Häder 2002; Weber 2005). Because our experimental condition also included some UVA and visible light radiation, data from this experiment potentially contain the effects of photoreactivation. Then, the ratio of UVA and visible lights in the spectrum was extremely smaller than those in solar radiation, suggesting that photoenzymatic repair is likely to play more effectively under solar radiation than our experimental condition. However, more details have never been studied. Whether eggs can be photoreactivated as well as adult females is also not known.

Consequently, our findings suggest that *T. urticae* is much more vulnerable than it was considered and photoreactivation plays an important role to survive UV radiation in *T. uritcae*. They escape from solar UV radiation by remaining on the underside of leaves (Sakai and Osakabe 2010). Moreover, Fukaya et al. (2013) reported the preferential exploitation of shaded area that was demonstrated in *Panonychus citri* (McGregore), an upper surface user of host plant leaves (Fukaya et al. 2013). To understand how mites cope with a solar UVB radiation threat to their survival and fitness, it is critical to assess both physiological and behavioral adaptation to ambient UVB radiation as well as the mechanisms causing UV damage and its repair.

In the next chapter, I verified the photoreactivation capacity in *T. urticae*, assuming that photoreactivation may be concerned with the divergence of UVB lethal effect between laboratory and field.

Section2: Investigation of UVB Effect of Extremely Low Intensity

- Materials and Methods

In order to clarify the damage threshold by the intensity of UVB radiation, I additionally tested the effects of weak UVB irradiation on egg hatchability. Low-intensity treatments were performed by irradiation with 0 (control) and 0.023 W m^{-2} for 10 h, 0 and 0.014 W m^{-2} for 217 min, and 0 and 0.018 W m^{-2} for 284 min and 471 min. For the low-intensity treatment, the overhead UVB lamp was covered with a black metal mask made of a perforated metal mesh [Perforated Metal No. 16 (φ2 × 3.5P staggered perforation; 29.6% open), Metaltech Co., Tokyo]. Two Petri dishes prepared using the same procedure described above were set on the shelf at 1.75 m from the UVB lamp, and another two Petri dishes were placed on the adjoining shelf as controls (0 W m^{-2}).

A series of treatments was performed once. The numbers of eggs used for each combination of UVB intensity and irradiation time length (two Petri dishes containing eight leaf disks) were 376–571.

After exposure to UVB radiation, egg hatchability was determined using the procedure described above. In the data analysis, mortality rates from the low- and high-intensity (described above) treatments were compared.

To evaluate whether reciprocity was applicable to the effects of low-intensity irradiation (0.014–0.023 W m^{-2}), I performed a generalized linear model (GLM; Gaussian) analysis using probit mortality data sets for eggs, with the UVB irradiation treatment categorically divided into low intensity and high intensity (0.19–0.58 W m^{-2}). The probit mortality data sets were obtained using the procedure described above.

- Results

The mortalities of eggs exposed to UVB radiation at low intensity (0.014–0.023 W m^{-2}) also increased with cumulative UVB irradiance and were distributed around the linear regression line for eggs exposed to UVB radiation at high intensity (0.19–0.58 W m^{-2}; Fig. 7). A GLM analysis revealed that the UVB intensity to which eggs were exposed (low or high) did not significantly affect egg mortality (Table 2), suggesting that reciprocity is also applicable when eggs are exposed to UVB radiation at very low intensity.

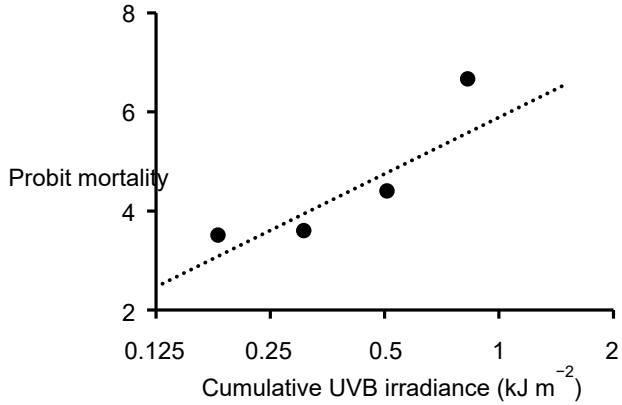

Fig. 7. Mortality of eggs exposed to UVB radiation at low intensity (0.014–0.023 W m^{-2}; solid circles) and regression line of eggs exposed to UVB radiation at high intensity (0.19–0.58 W m^{-2}; dotted line; see Table 2).

Table 2. GLM analysis for applicability of reciprocity to UVB irradiation at low intensity (0.014–0.023 W m^{-2}) [probit mortality ~ ln(x) + UVB intensity (high/low)]

	Coefficient	SE	*t*-statistic	Pr(>|t|)
(Intercept)	5.9138	0.1448	40.839	$< 2 \times 10^{-16}$
ln(x)[a]	1.6972	0.1506	11.270	1.01×10^{-8}
UVB intensity (low)	0.2201	0.2749	0.801	0.436

[a] Logarithmic cumulative UVB irradiance

Discussion

Divergence from the reciprocity law was observed in aquatic animals under UVB radiation at low intensity such as 0.2–0.4 W m^{-2} (Cywinska et al. 2000; Wübben 2000), suggesting a presence of damage threshold by UVB intensity. In contrast, reciprocity was applicable to mortality of *T. urticae* eggs even if those were exposed to very low-intensity UVB radiation (0.014–0.023 W m^{-2}). Instead, I found damage threshold cumulative UVB irradiances for juvenile performance; the developmental rate was not affected by UVB irradiation below 0.5 kJ m^{-2}. Therefore, I concluded that the reciprocity law is applicable to UVB damage in *T. urticae*. This may be the first report demonstrating the reciprocity law for UVB damage in a terrestrial animal. Such difference in thresholds between aquatic and terrestrial animals might be caused by the difference in the presence/absence of surrounding water.

Section3: Variation of UVB Vulnerability during Embryogenesis

- Materials and Methods

Four Petri dishes were prepared using the same procedure described above. After counting the laid eggs on Petri dishes, these were kept in laboratory chamber (25°C, 16:8 h L:D). These preparations were continuously treated every other day for 4 days. On the fifth day, just after removing adult females which were introduced on the day before, all eggs were exposed to UVB irradiation for 1h. Then, the eggs of 0 to 3 days old on each Petri dish were simultaneously irradiated by UVB. During irradiation, four Petri dishes sets containing the eggs of 0 to 3 days old were then placed on three shelves for irradiation at 0.19, 0.31, and 0.58 W m^{-2} of UVB radiation, respectively, and the remaining one set was placed on the adjoining shelf as controls (0 W m^{-2}).

This series of treatments was performed once. The numbers of eggs on each prepared dish (containing eight leaf disks) were 30–84 in total (174–285 eggs per leaf disk).

After exposure to UVB radiation, the Petri dishes were returned to the laboratory where they had been reared before treatment (25°C, 16:8 h L:D). Hatchability was checked on day 6 after removing adult females, respectively. Since a few of emerged larvae were observed just before UVB irradiation in the eggs of 3 day old, I irradiated UVB after removing the emerged larvae and confirmed no larvae were emerged during UVB irradiation.

- Results

Hatchability largely varied with the day age. The 1 day age eggs were most sensitive to UVB (Fig. 8). On the irradiation of 0.19 and 0.31 W m^{-2}, the hatchability of the 2 day age eggs was increased remarkably and the 3 day age eggs hatched still more under the 0.19 W m^{-2} irradiation treatment. In contrast, on the 0.31 W m^{-2} irradiation treatment, the 3 day age eggs hatched less than the 2 day age eggs. Although the eggs of the 0 to 2 day age hardly hatched, ~16% hatchability was observed on the 3 day age eggs under the 0.58 W m^{-2} irradiation treatments.

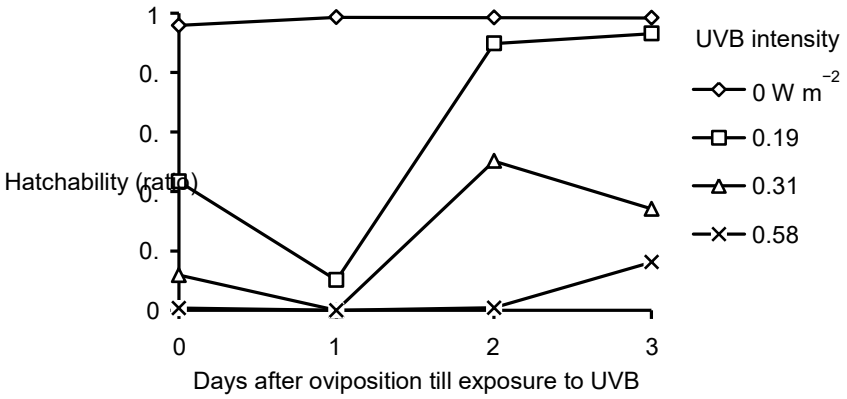

Fig. 8. Age (days after oviposition) dependent variation in hatchability of *T. urticae* eggs after UV-B exposure.

- Discussion

The eggs 1 day after oviposition (24–48h after oviposition) were most vulnerable to UVB for egg duration. As for embryogenesis, *T. urticae* eggs 1 day after oviposition were roughly at the stage in which the larval body is formed based on the germinal disk under 25°C condition (Dearden et al. 2002). Therefore, UVB might affect particularly some physiological mechanisms. As mentioned above, chrysalis stages are also more vulnerable to UVB. In both eggs and chrysalis, variation of UVB sensitivity is possibly concerned with physiological mechanism to develop for next stage. In order to make clear the relation between UVB vulnerability and embryogenesis, more detailed verification is required.

Chapter4: Photoreactivation in *T. urticae*

The reciprocity law was applied in UVB-induced mortality in *T. urticae*. However, the LD_{50} value for eggs exposed to artificial UVB (laboratory, 0.58 kJ m^{-2}; Murata and Osakabe 2013) is lower than that elicited by solar UVB radiation (~50 kJ m^{-2}; Sakai et al. 2012).

UVB radiation causes DNA damage in organisms, including the formation of pyrimidine dimers such as cyclobutane pyrimidine dimers (CPD) and pyrimidine (6-4) pyrimidone photoproducts. To avoid the harmful effects of UV-induced DNA damage, organisms have two major DNA repair mechanisms: excision repair (dark repair pathways: base excision repair and nucleotide excision repair) and photo-enzymatic repair (PER; Malloy et al. 1997). Excision repair is a multiple enzyme system that replaces the damaged DNA with new, undamaged nucleotides using energy derived from ATP (Sinha and Häder 2002). In PER, DNA lesions are directly repaired by a photolyase using energy from blue visible light (400-450 nm wavelength; Sancar 2003) and ultraviolet-A (UVA; 315-400 nm wavelength; Kalthoff 1975; Shiroya et al. 1984; Sinha and Häder 2002).

As solar radiation includes intense visible light, I assumed that a photoreactivation mechanism would play a role in the survival of *T. urticae* under solar radiation, causing a difference between laboratory and outdoor experiments.

Assessed the capacity for photoreactivation in *T. urticae* eggs, I found the photoreactivaiton efficacy. Egg hatchability exposed to visible light after UVB irradiation increased much more than that kept under dark condition after UVB irradiation (Fig. 9; hatchability on +VIS: 64.8%; −VIS: 13.0%). Then, I examined some factors affecting photoreactivation in eggs and larvae.

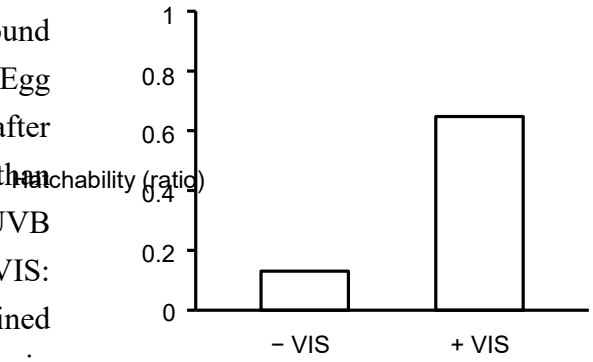

Fig. 9. Hatchability of *T. urticae* eggs 6 days after exposure to UVB radiation. "− VIS" represent the hatchability of eggs irradiated with UVB (0.16 W m^{-2}) for 30 min and kept under dark condition. "+ VIS" represent the hatchability of eggs additionally irradiated with visible light (VIS: 67.7 W m^{-2}) for 90 min after exposure to UVB radiation for 30 min.

Section1: Dose-response in Egg Photoreactivation

- Materials and Methods

Four kidney bean leaf squares (2 × 2 cm) were placed on water-soaked cotton in each of two Petri dishes (9 cm in diameter). Five adult *T. urticae* females were introduced onto each leaf disk. The females were allowed to oviposit for 24 h in a laboratory at 25°C under a 16-h light: 8-h dark (16L:8D) photoperiod. Then, the females were removed and the eggs laid on the leaf disks were counted. These Petri dishes were placed on a shelf in a darkened growth chamber and immediately exposed to UVB radiation. A Petri dish assigned to be the dark control (without photoreactivation) was placed inside a cardboard box (dark box: 24.0 × 16.5 × 10.8 cm) immediately after UVB irradiation.

The dark box with the dark control inside and the other Petri dish (photoreactivation treatment) were set on a shelf and exposed to VIS (halogen lamp) using various combinations of intensities and times; 21.6 W m^{-2} for 40, 80, 120, 160, or 210 min (the cumulative irradiances were 51.8, 104, 156, 207, and 272 kJ m^{-2}, respectively); 36.8 W m^{-2} for 20, 40, 60, 100, or 140 min (44.2, 88.3, 132, 221, and 309 kJ m^{-2}, respectively); 67.7 W m^{-2} for 10, 20, 30, or 60 min (40.6, 81.2, 122, and 244 kJ m^{-2}, respectively); and 142 W m^{-2} for 8, 15, 20, 25, or 35 min (68.2, 128, 170, 213, and 298 kJ m^{-2}, respectively).

The voltage provided to the halogen lamps was reduced using a variable autotransformer to achieve irradiances < 67.7 W m^{-2} (100 V) (Fig. 2b). An irradiance of 142 W m^{-2} was accomplished by lifting the Petri dishes to 23 cm above the shelf [44 cm from the halogen lamps (100 V)] using a jack.

After treatment, the Petri dishes, including the photoreactivation treatments and dark control, were immediately placed inside a larger cardboard box (34.5 × 37.8 × 13.5 cm) together in the dark until subsequent observation. The cardboard box was placed in the laboratory at 25°C. Egg hatchability was checked on day 6 after exposure. I preliminarily confirmed that few eggs hatched later than 6 days post-exposure. This series of treatments was replicated twice. A total of 80–371 eggs/Petri dish (replicate) were used in our experiments.

The photoreactivation efficiency was calculated using formula (2) (Kelner, 1951):

$$S = \frac{Y - X}{1 - X} \quad (2)$$

where S, X, and Y represent the photoreactivation efficiency, egg hatchability of the dark

control, and hatchability of eggs exposed to VIS (photoreactivated), respectively, in each replicate. The effects of VIS intensity, time of VIS irradiation, and cumulative VIS irradiance on the photoreactivation efficiency (*S*) were evaluated by the stepwise model selection method with the generalised linear model (GLM) based on Akaike's information criterion (AIC) using the "stepAIC" module in the "MASS" package of R software ver. 3.0.0. Next, the function expected between *S* and the cumulative VIS irradiance (see Results) was fitted using the nonlinear least-squares method, and pseudo standard errors of the estimated parameters were calculated using the "nlm" module in the "stats" package and "sqrt" module in R software, respectively. I calculated 95% confidence intervals (CIs) for the predicted regression line based on the pseudo standard errors.

The average egg hatchability for the dark control over all replications and its CI were estimated using the "qt" module in R software after an arc sin root transformation.

- Results

The average egg hatchability over all replications for the dark control was 0.106 (95% CI, 0.096–0.116). The stepwise model selection supported a model including only the cumulative VIS irradiance (AIC = 42.24; AIC = 68.83 in the null model). Thus, the photoreactivation effects were determined by the cumulative VIS irradiance, obeying reciprocity. However, the function of the cumulative VIS irradiance in the photoreactivation efficiency was nonlinear; it increased slowly around the origin, linearly in the next, and then levelled off at higher cumulative irradiances (Fig. 10). This pattern was similar to the logistic curve, but its saturation point did not reach 1. Therefore, the following model (3) was fit to the relationship between the cumulative VIS irradiance and the photoreactivation efficiency using a nonlinear least-squares method:

$$(3), \qquad y = \frac{ae^{(b+cx)}}{1+e^{(b+cx)}}$$

where y and x represent the photoreactivation efficiency and the cumulative VIS irradiance, and a, b and c are constants. The constants were calculated to be 0.57025971, −3.56120355 and 0.04089434 for a, b and c, respectively (Fig. 10; minimum = 0.2635581), indicating that up to 57% of the eggs were reactivated due to photoreactivation from UVB damage.

Consequently, the survival ratio of eggs through photoreactivation (maximum, 0.570) and dark repair pathways (or potentially not vitally damaged; 0.106) after UVB

irradiation at 0.288 kJ m^{-2} was estimated to be maximum of 0.676.

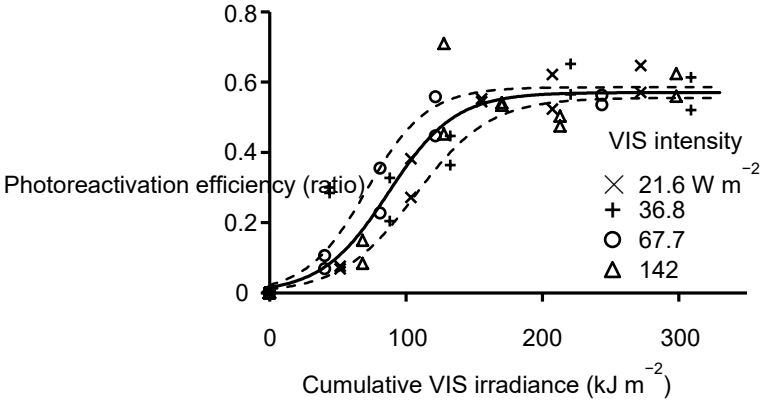

Fig. 10. Effects of cumulative VIS irradiance on egg photoreactivation. The solid line is the regression curve fitted by a nonlinear least-squares method using formula (3). Dashed lines represent the 95% CI range.

- Discussion

The increase in egg hatchability in *T. urticae* induced by photoreactivation depended on the cumulative VIS irradiance with no regard to intensity, indicating reciprocity. However, the photoreactivation efficiency in *T. urticae* eggs leveled off. This indicates that all of eggs exposed to UVB couldn't survive deleterious UVB effects by photoreactivation. The phase-specific vulnerability for egg duration shown in previous chapter might be concerned with reaching the limit of hatchability.

The survival ratio after maximum photoreactivation was 0.676 with UVB irradiation of 0.288 kJ m^{-2}. This survivorship was lower than the estimated hatchability of 0.877 at 0.288 kJ m^{-2} calculated from the cumulative irradiance–mortality regression line in Section1 of Chapter3. In that experiment, photoreactivation was probably caused during UVB irradiation and enabled more eggs to survive UVB radiation since the eggs were irradiated with UVB in a laboratory illuminated with fluorescent lamps.

Section2: Time Lag Effect between UVB and VIS Irradiation on Egg

- Materials and Methods

Eggs

T. urticae eggs in five Petri dishes with four kidney bean leaf squares (2 × 2 cm) were prepared as dose-response experiments, and all dishes were exposed to UVB radiation. Then, one Petri dish was successively exposed (LAG0) to VIS radiation at an intensity of 67.7 W m^{-2} for 90 min (cumulative irradiance: 366 kJ m^{-2}; photoreactivation treatment). Three of the remaining four dishes were also exposed to VIS radiation under the conditions described above, but at 1, 2, or 4 h after the end of UVB irradiation (LAG1, LAG2, or LAG4; delayed photoreactivation treatment). The last dish was never exposed to VIS radiation (VIS−; dark control). All Petri dishes were kept inside a cardboard dark box after UVB irradiation except when exposed to VIS radiation.

The hatchability of the eggs was checked under a binocular microscope, every day (10 min to observe each Petri dish) until day 6 after exposure. Although the dark condition was briefly broken during these observations, I tentatively confirmed that VIS irradiation later than 24 h did not cause photoreactivation (Fig. 11). Each series of treatments was performed twice. The number of eggs used in our experiments was 172–281 per Petri dish (replicate).

I transformed the hatchability on day 6 for each replicate to an empirical logit (*EL*) using the following formula to compare the egg hatchability among the delayed photoreactivation treatments and dark control:

$$EL = \ln\left(\frac{x+0.5}{n-x+0.5}\right) \quad (4),$$

where x and n represent the number of eggs hatched and the total number of individuals tested. The *EL*s were applied to Bartlett's test for homogeneity of variances using the "bartlett.test" module in R software. Multiple comparisons by Tukey's HSD method were performed using the "TukeyHSD" module following a one-way analysis of variance (ANOVA) with the "aov" module in R software.

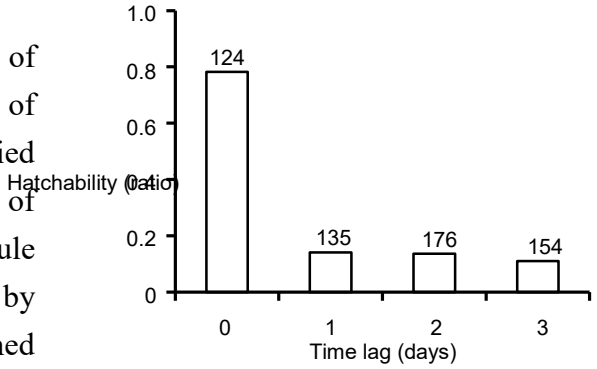

Fig. 11. Effects of time lag between UVB and VIS radiation on photoreactivation in *T. urticae* eggs. A figure above each bar represent the number of eggs tested.

- Results

Bartlett's test did not reject the homogeneity of variances among the immediate (LAG0) and delayed photoreactivation treatments (LAG1, LAG2, and LAG4) or the dark control (VIS−) in the *EL* transforms (P = 0.8958). A one-way ANOVA revealed significant differences in egg hatchability among the treatments and control ($F_{[4,5]}$ = 66.76, P = 0.000158). The photoreactivation efficiency was reduced as the time lag between UVB and VIS irradiation increased; the percentage of eggs showing reactivation was 62.5% (57.6–67.3%) and 2.7% (2.3–3.2%) in LAG 0 and LAG4, respectively (Tukey's HSD method, $P < 0.05$; Fig. 12). Eventually, no photoreactivation efficacy was detected in LAG4 compared with VIS− (Tukey's HSD, $P > 0.05$; Fig. 12).

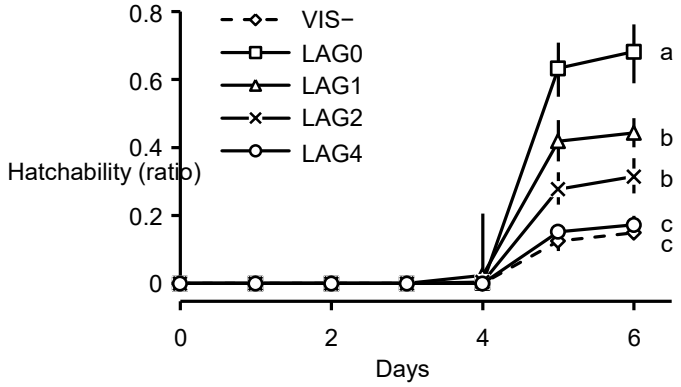

Fig. 12. Effects of a time lag between UVB and VIS irradiation on egg photoreactivation. Different letters represent significance (Tukey's HSD, P < 0.05). VIS−, dark control; LAG0, without a time lag; LAG1, 1-h time lag; LAG2, 2-h time lag; and LAG4, 4-h time lag. The vertical lines in each plot represent the 95% CI range.

- Discussion

The photoreactivation efficiency decreased with an increasing time lag between UVB irradiation and VIS irradiation; however, no reactivation effects were observed when the time lag was 4h (LAG4). I tentatively determined that eggs aged 24–48 h after oviposition were the most vulnerable to UVB radiation for the egg duration (Section3 of Chapter3). Probably, in the case of LAG4, most eggs had already developed into that phase before VIS irradiation and VIS exposure treatment may become too late to restore physiological control. To reveal this hypothesis, more detailed observation and physiological analysis are required.

Section3: Photoreactivation in Larva

- Materials and Methods

Two kidney bean leaf squares (2 × 2 cm) were placed on water-soaked cotton in each of seven Petri dishes. Five adult *T. urticae* females were introduced onto each leaf disk and allowed to oviposit for 24 h in the laboratory (25°C, 16L:8D). After the adult females were removed, the Petri dishes were covered with transparent plastic lids to raise the relative humidity on the leaves. This treatment delays hatching under extremely high humidity until the humidity falls (Ubara and Osakabe 2015). A similar suspension of development caused by extremely high humidity was reported in *T. urticae* from teleiochrysalises to adults (Ikegami et al. 2000). Four days later (day 0), the lids were opened and most of the eggs hatched within 30 min. Larvae that had emerged before the lids were opened were removed. I counted the number of emerged larvae 2 h later, and six of the seven Petri dishes were immediately exposed to UVB radiation. The remaining Petri dish was assigned as the dark control without exposure to UVB (UVB− dark control) and was kept in a cardboard dark box while the other Petri dishes were exposed to UVB radiation and subsequent VIS irradiation.

After UVB irradiation, each Petri dish was subjected to photoreactivation treatment or used as a dark control with exposure to UVB (UVB+ dark control). One Petri dish was exposed to VIS radiation for 90 min (366 kJ m^{-2}) immediately after UVB irradiation (LAG0), and each of the four dishes were irradiated with VIS 1, 2, 3, or 4 h later (LAG1, LAG2, LAG3, or LAG4). All Petri dishes were kept inside the cardboard dark box after UVB irradiation except when exposed to VIS radiation.

The status of the mites (living/dead, developmental stage) was recorded on the next day (day 1) and day 8. The observations took 10 min per Petri dish. Each series of treatments was performed twice. The number of larvae used for treatment was 43–94 per Petri dish (replicate).

To evaluate the effects of VIS radiation and the time lag from UVB to VIS irradiation on larval development and survival, I transformed the ratio of individuals that had developed into a protochrysalis (the developmental stage following larva; day 1) or survived (developed to adulthood; day 8) in each replicate to an *EL* using formula (4). The *EL*s were applied to Bartlett's test for homogeneity of variances, a one-way ANOVA, and a post-hoc test with Tukey's HSD method using the "bartlett.test," "aov," and "TukeyHSD" modules in R software.

- Results

The homogeneity of variances in the *EL*s for development to a protochrysalis (day 1) and survival to adulthood (day 8) was supported among the immediate and delayed photoreactivation treatments and dark controls with and without UVB exposure by Bartlett's tests (day 1, $P = 0.7269$; day 8, $P = 0.5771$). All individuals in all treatments survived on day 1, and 94.6% of individuals in the UVB− dark control developed to a protochrysalis (Table 3). In contrast, all individuals remained at the larval stage in the UVB+ dark control (Tukey's HSD, $P < 0.05$), and they looked healthy. Although no significant differences from the UV− dark control were detected by Tukey's HSD method ($P > 0.05$), exposure to UVB radiation with photoreactivation with or without a time lag was likely to delay the development of larvae to protonymphs; up to 70% of individuals had developed to a protochrysalis on day 1.

In the UVB− dark control, 97.8% of individuals survived and developed to adulthood, whereas individuals in the UVB+ dark control died by day 8 (Tukey's HSD, $P < 0.05$; Table 3). Most individuals in the UVB+ dark control died at the protochrysalis stage or during the moulting period. Up to 96.4–100% of individuals subjected to photoreactivation with and without a time lag developed (survived) to adulthood, which is not different from that in the UVB− dark control (Tukey's HSD, $P > 0.05$; Table 3).

Table 3 Survival and development of *T. urticae* once exposed to UVB radiation at larval stage.

	Day 1			Day 8	
Treatment[a]	No. of larvae (mean±SE)	Survival ratio	Ratio of individuals developed to protochrysalis (CI)[b]	No. of individuals (mean±SE)	Survival ratio to adulthood (CI)[b]
UV−dark	64.0±1.0	1.00	0.946 (0.931–0.958) a	45.0±20.0[c]	0.978 (0.924–0.999) a
LAG0	74.0±8.0	1.00	0.701 (0.490–0.852) a	74.0±8.0	0.989 (0.868–1.00) a
LAG1	60.0±4.0	1.00	0.703 (0.275–0.941) a	59.5±4.5	1.00 (0.999–1.00) a
LAG2	67.0±13.0	1.00	0.657 (0.468–0.807) a	67.0±13.0	0.990 (0.952–1.00) a
LAG3	83.5±10.5	1.00	0.547 (0.354–0.727) a	83.5±10.5	0.978 (0.926–0.997) a
LAG4	69.5±8.5	1.00	0.592 (0.461–0.712) a	69.5±8.5	0.964 (0.932-0.983) a
UV+dark	52.0±9.0	1.00	0 b	52.0±9.0	0 b

[a] UV−dark: dark control without exposure to UVB (UVB− dark control), LAG0: larvae exposed to VIS radiation immediately after UVB irradiation was finished, LAG1–4: larvae with 1–4 h time lag between exposure to UVB and VIS, UV+dark: dark control with exposure to UVB (UVB+ dark control).

[b] To calculate mean and 95% CI, I used empirical logit transforms. Different letters at the right side of columns represent statistical differences shown in a post hoc test following one-way ANOVA (TukeyHSD, $P < 0.05$).

[c] One of two leaves in a replicate (Petri dish) was omitted because deterioration.

- Discussion

Unlike eggs, a 4-h time lag did not affect the efficiency of larval photoreactivation. In larvae, the survivability after UVB irradiation at 0.288 kJ m^{-2} was predicted to be 0.9996 from the linear regression line (Section1 of Chapter3); this corresponds with the results for photoreactivated larvae in this experiment.

All of the larvae exposed to UVB were alive after 24 h (day 1), regardless of whether VIS was irradiated or not. Nevertheless, none of the larvae that were not photoreactivated (UVB+ dark control) developed into a protochrysalis. Most individuals in the UVB+ dark control died at the protochrysalis stage or at moulting. The same phenomena were observed in a previous experiment where larvae exposed to UVB radiation died primarily during the protochrysalis stage or later when failing to moult to protonymphs (Section1 of Chapter3). The physiological systems for ecdysis are likely to be vulnerable to UVB damage, and vulnerability during the chrysalis stage may vary depending on the phase preceding moulting.

The observed time lag effects in eggs and larvae indicate that mites exposed to UVB radiation sicken at particular developmental phases such as the phase from germinal disk formation through embryonic development and ecdysis phase of the chrysalis stage. I hypothesized that UVB-induced DNA damage obstruct physiological control at a particular phase of embryogenesis or ecdysis, and mites survive UVB radiation if PER repair the damage before those phases. To demonstrate this hypothesis, detailed molecular analysis is necessary.

Section4: Effects of Wavelength-filtered VIS and UVA on Egg Photoreactivation

- Materials and Methods

Two Petri dishes containing four kidney bean leaf squares (2 × 2 cm) with *T. urticae* eggs were prepared using the same procedure as in the dose-response experiments described above, and both Petri dishes were exposed to UVB radiation. Next, one Petri dish was placed inside a dark cardboard box, while the other was exposed to wavelength-filtered light or UVA radiation for 30 min. During irradiation, the Petri dishes assigned for exposure to wavelength-filtered light were placed in a cardboard box (22.5 × 12.0 × 5.20 cm) with a top covered with coloured cellophane film (Toyo, Tokyo,

Japan) and illuminated with halogen lamps through the film. The cumulative irradiance values of the filtered lights were 85.5, 88.5, 83.3, and 86.3 kJ m^{-2} for blue (irradiance: 47.5 W m^{-2}), green (49.2 W m^{-2}), yellow (without jack; 46.3 W m^{-2}), and red (47.9 W m^{-2}) light, respectively (Fig. 2c). For UVA irradiation, a UVA handy lamp (29.1 W m^{-2}; UVL-56 Handheld UV Lamp; UVP, Cambridge, UK) was used to test the photoreactivation effects caused by UVA irradiation. UVA irradiance was measured using an irradiance meter ($X1_1$) equipped with a UV-3701-4 detector head (Gigahertz-Optik GmbH). The cumulative irradiance value of UVA was 52.4 kJ m^{-2} (Fig. 2d).

After radiation exposure, all Petri dishes were placed inside a dark cardboard box and checked for egg hatchability using a binocular microscope on day 6. The series of treatments was replicated twice. A total of 188–284 eggs were used per Petri dish (replication).

I transformed the egg hatchability value (ratio) for each replicate to an *EL* using formula (4) to compare the effects of wavelength-filtered VIS and UVA irradiation on photoreactivation. The *EL*s were applied to Bartlett's test for homogeneity of variances, a one-way ANOVA and a post-hoc test with Tukey's HSD method using the "bartlett.test," "aov," and "TukeyHSD" modules in R software.

- Results

The homogeneity of variances in the *EL*s for hatchability was marginally supported among all treatments, including the dark controls (Bartlett's tests, $P = 0.05832$). I confirmed the homogeneity of variances in the *EL*s among all treatments, excluding the dark controls (Bartlett's tests, $P = 0.1499$). A one-way ANOVA (including the dark controls) showed a significant difference in hatchiability among treatments ($F_{[9,10]} = 39.03$, $P = 1.28\times10^{-6}$). UVA, blue, and, green lights exhibited substantial photoreactivation effects in comparison with the dark control (Tukey's HSD, $P < 0.05$; Fig. 13). In contrast, no effects were detected following treatment with yellow and red light, in which the egg hatchability was not significantly different from that in the dark controls (Tukey's HSD, $P > 0.05$; Fig. 13).

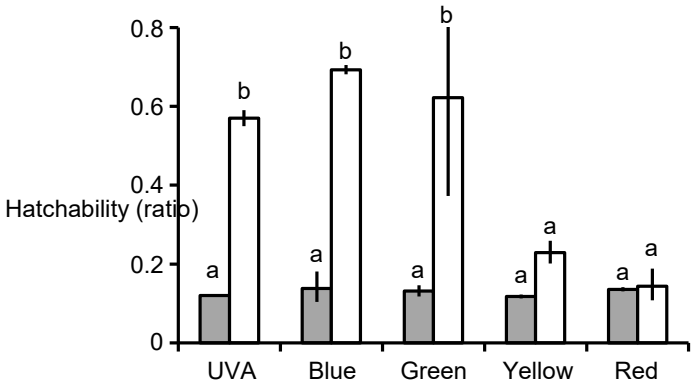

Fig. 13. Effects of wavelength-filtered VIS and UVA on egg photoreactivation. White bars represent the hatchability of eggs exposed to VIS and UVA after exposure to UVB radiation. Grey bars represent the hatchability of eggs exposed to UVB without photoreactivation (dark control). The vertical line at the top of each bar shows the 95% CI range. Different lowercase letters indicate significant differences in hatchability (Tukey's HSD, $P < 0.05$).

- Discussion

Radiation of 350–450 nm is generally effective for photoreactivation (Rupert 1975; Sancar 2003). PER activity peaks with radiation of 375 and 436 nm in *E. coli* and *S. griseus*, respectively (Kelner 1951), 430–450 nm in the cyanobacteria, *Agmenllum quadruplicatum* (Baalen and O'Donnell 1972), 440 nm in *Smittia* sp. (Kalthoff et al. 1978), and 366 nm in *P. tridactylus* (Chiang and Rupert 1979). The wavelengths effective for photoreactivation in *T. urticae* correspond roughly with these general trends; radiation in the range from UVA to green (≤ 500 nm) was effective. Additional detailed studies are required to elucidate the PER action spectra in spider mites.

Chapter5: Photo-enzymatic Repair of UVB-induced DNA Damage in *T. urticae*

Although UVB radiation potentially exerts various effects on organismal cells, the most important target may be DNA (Peak et al. 1984; Sinha and Häder 2002). UVB-induced DNA lesions are caused by the formation of cyclobutane pyrimidine dimers (CPDs) and 6-4 pyrimidine-pyrimidine photoproducts (6-4PPs) (Britt 1996; Sinha and Häder 2002); in general, the former and latter comprise 75% and 25% of DNA lesions, respectively (Mitchell and Nairn 1989). Two enzymatic repair mechanisms, nucleotide excision repair (NER) and photo-enzymatic repair (PER), of UV-induced DNA lesions are well known. NER is a complex system composed of many enzymes working without regard to photo energy (Gillet and Schärer 2006). Briefly, the damaged DNA region is excised, and the gap is filled by DNA polymerase. In contrast, during PER, DNA lesions are repaired directly by photolyase using light energy (photoreactivation; Sancar 2003). Photolyases are categorized into CPD photolyase and (6-4) photolyase, which specifically bind to CPDs and 6-4PPs, respectively. (6-4) photolyase PER function is absent in placental mammals (Sinha and Häder 2002; Karentz 2015). In fact, humans do not possess photolyase (Li et al. 1993; Thoma 1999; Sancar 2003).

Photoreactivation has been demonstrated in spider mites (Santos 2005; Murata and Osakabe 2014; Suzuki et al. 2014) and phytoseiid mites (Murata and Osakabe unpublished). In fact, the LD_{50} values of the two-spotted spider mite, *Tetranychus urticae* Koch, due to solar UVB radiation were 86-fold higher than those due to a UVB lamp in the laboratory (Sakai et al. 2012; Murata and Osakabe 2013), suggesting that photoreactivation plays a significant role in survival under field conditions.

Studies on the biological impacts of UVB radiation and photoreactivation are abundant in aquatic arthropods (Kouwenberg et al. 1999b; Zagarese et al. 1997; Wübben 2000; Connelly et al. 2009). In contrast, similar studies in terrestrial animals are rare, and thus the physiological mechanisms remain largely unknown and/or unverified. In this chapter, I attempted to show DNA lesions generated by UVB irradiation and the reduction of those lesions by the action of PER in spider mites. First, I quantified CPDs and 6-4PPs induced by UVB irradiation and evaluated the reduction of DNA lesions by PER and NER under light and dark conditions, respectively, in *T. urticae*. To evaluate the role of photo enzymatic repair, I analysed the interaction between the DNA lesion amount and the gene expression level of CPD photolyase. Furthermore, that of the xeroderma pigmentosum group A (XPA) protein which is one

of the core factors of NER was evaluated. In NER, XPA binds damaged DNA after damage recognition. It takes a role of reaction to form an open complex of DNA for replacement with new nucleotides at relatively initial stage of multiple NER reactions (Gillet and Schärer 2006). By evaluation of this gene, the potential effect of NER associated with UVB and VIS irradiation was verified.

Section1: DNA Damage Detection about UVB Irradiation and Photoreactivaitgon in Larva

- Materials and Methods

DNA damage detection in UVB-irradiated larvae

A kidney bean leaf disk (5.0 × 5.0 cm) was placed on water-soaked cotton in each of 10 Petri dishes. Fifteen adult *T. urticae* females were introduced onto each leaf disk. These Petri dishes were maintained for 24 h in the chamber (25°C, 16 L:8 D); thus, females were allowed to oviposit for 24 h. After 24 h, adult females were removed, and the Petri dishes were covered with transparent plastic lids to raise the relative humidity on the leaves. This treatment delays hatching until the humidity falls (Ubara and Osakabe 2015). Four days later, the lids were opened and almost all of the eggs hatched within 2 h.

Twelve kidney bean leaf squares (0.5 × 0.5 cm) were placed on water-soaked cotton in each of four Petri dishes, and within 5 h after hatching, *T. urticae* larvae were introduced onto the leaf disks (one larva per leaf disk) using a fine brush. Furthermore, a piece of polyester film (HB3 polyester film, 25 μm thick; Teijin DuPont Films; 0.8 × 2.0 cm) was placed on the centre of the water-soaked cotton in the same Petri dish. Within 5 h after hatching, larvae were introduced onto the film (100 larvae per film) using a fine brush. Three of the four Petri dishes were exposed to UVB irradiation, and each was assigned to exposure times of 10, 20 or 30 min (UVB10, UVB20 and UVB30 treatment, respectively). Simultaneously, the remaining single Petri dish was placed in a cardboard box and placed in the same irradiation chamber for 30 min (dark control). After the irradiation treatments, the films containing UVB-irradiated larvae were immediately placed into a 1.5-mL micro tube (Eppendorf) containing 450 μl lysis buffer solution [10 mM Tris-HCl (pH 8.0), 10 mM EDTA and 0.5% sodium dodecyl sulfate]. The larvae were homogenised with pellet mixer, and 4.5 μl Proteinase K (10 mg mL^{-1}; Takara bio Inc.) were added to the lysate. Then, the lysate was incubated at 65°C for 10

min in a water bath. After incubation, 450 µl phenol/chloroform/isoamyl alcohol (25:24:1) (Sigma-Aldrich) were added to the lysate and incubated at room temperature with stirring by a rotator (Taitec Inc.) twice for 30 min. To remove the remaining phenol in the samples, samples were extracted with 800 µl diethyl ether twice. RNA in the samples was digested with 4.5 µl RNase A (1 mg mL^{-1}) (QIAGEN) at 37°C for 30 min in a water bath and then extracted again with phenol/chloroform/isoamyl alcohol and diethyl ether. DNA in the resulting samples was precipitated by adding ethanol after the addition of 0.1 volumes of 3 M sodium acetate. After centrifugation, the DNA pellets were dissolved with 20 µl 1 × TE buffer. The quantity and quality of the resulting DNA samples were evaluated using a spectrophotometer (NanoDrop Lite Sp, Thermo Scientific Inc.). Then, the DNA samples were examined for UV-induced DNA damage detection. Each series of treatments was performed in three replicates. UV-induced CPDs and 6-4PPs in the DNA samples were quantified by enzyme-linked immunosorbent assay (ELISA) using the High Sensitivity CPD/Cyclobutane Pyrimidine Dimer ELISA kit with a TDM-2 monoclonal antibody (Cosmo Bio Co., Ltd.) and the High Sensitivity 6-4PP/(6-4)Photoproducts ELISA kit with a 64M-2 monoclonal antibody (Cosmo Bio Co., Ltd.), following the manufacturer's instructions. Briefly, denatured sample DNA (CPD detection: 20 ng/well; 6-4PP detection: 130–200 ng/well) was added in 96-well protamine sulfate-coated flat-bottomed microtiter plates (Cosmo Bio Co., Ltd.). The binding of TDM-2 antibodies to CPD and 64M-2 antibodies to 6-4PP were detected by sequential treatment of wells with biotinylated secondary antibodies, streptavidin-peroxidase and o-phenylenediamine (OPD). The absorbance of coloured products derived from OPD, which is the strength generally proportional to the amount of TDM-2 antibody and 64M-2 antibody remaining bound to the plate, were respectively measured at 492 nm using a microplate reader (Corona electric Co., Ltd.). The standard dose-response curve was calculated by the absorption of UVC-irradiated DNA samples, which were calf thymus DNA irradiated by various doses of UVC (0, 2.5, 5, 7.5 and 10 J/m^2) (Cosmo Bio Co., Ltd.). UVC-irradiated DNA samples were commonly used as standard in damage detection (Berton and Mitchell 2012). DNA damage in *T. urticae* samples was relatively quantified by applying the resulting absorptions to the standard curve in each replicate. To evaluate the effect of UVB on DNA lesion formation, linear regression analyses were performed for interactions between frequency of CPDs (or 6-4PPs) and UVB cumulative doses using the "lm" module in R software (version 3.1.0; R Development Core Team, 2014). The 95% confidence interval of the linear regression was calculated based on the 97.5% point of

cumulative probability distribution in the t-distribution predicted using the ‘‘qt’’ module in R.

After irradiation treatment and DNA sample collection, 12 larvae on each leaf disk were kept in a dark chamber (25°C, 0 L:24 D) and observed until all individuals died or progressed to adulthood. Observation of each treatment was conducted under light condition less than 5 minutes every day. To evaluate the effect of UVB dose on survival rate, generalised linear model (GLM; Binomial) analysis was performed using the “glm” module in R.

DNA damage repair in photoreactivation treatment.

T. urticae larvae on leaf disks and polyester film in eight Petri dishes were prepared as described above, and all dishes were exposed to UVB irradiation for 30 min. Then, four Petri dishes were continuously exposed to VIS irradiation for 5, 10, 20 or 30 min (+PR5, +PR10, +PR20 or +PR30 treatments, respectively). Simultaneously, the other four dishes were placed in a chamber and covered with a cardboard box to maintain dark conditions for 5, 10, 20 or 30 min (−PR5, −PR10, −PR20 or −PR30 treatments, respectively). These continuous irradiation treatments were conducted on the same day. After the irradiation treatments, larval DNA was extracted, and UV-induced CPD and 6-4PP were detected using the same procedures as in DNA damage detection in UVB-irradiated larvae. Each series of treatments was performed in three replicates.

To evaluate the DNA damage repair by each irradiation treatment, the CPD/6-4PP level in the UVB30 treatment was set as the baseline. The damage level seen with the UVB30 treatment was defined as 100% damage, of which all values presented here were calculated as percentages.

To evaluate the effect of VIS irradiation and the time course after UVB irradiation on the calculated percentage of remaining CPD and 6-4PP, the generalised linear mixed model (GLMM), in which repeated data have random effects, was constructed using the “lmer” module in the “lme4” and “lmerTest” package in R.

After irradiation treatment and DNA sample collection, 12 larvae on leaf disks were kept in a dark chamber (25°C, 0 L:24 D) and observed until all individuals died or progressed to adulthood. To evaluate the effect of VIS irradiation and the time course after UVB irradiation on survival rate, the GLMM, in which repeated data have random effects, was constructed using the “glmer” module in the “lme4” package in R.

- Results

DNA damage detection in UVB-irradiated larvae.

The survival rate decreased as the UVB cumulative dose increased (GLM, $P = 3.05 \times 10^{-9}$; Fig. 14a). Nearly all individuals were dead after 30 min of UVB irradiation. Larvae that ultimately died due to damage from UVB irradiation still appeared normal during the active larval stages after treatment. Most damaged individuals died at the next developmental stage, protochrysalis, by failing to moult and developmentally halting. These results are consistent with the results of Murata and Osakabe (2014).

The CPD frequency increased with the UVB cumulative dose. A significantly positive linear relationship between CPD quantity and UVB cumulative dose was observed (y=0.00256x, R^2=0.7997, P=2.288 × 10^{-5}; Fig. 15A). The 6-4PP frequency also significantly increased with UVB dose (y=0.01314x, R^2=0.5728, P=1.044 × 10^{-3}; Fig. 15B).

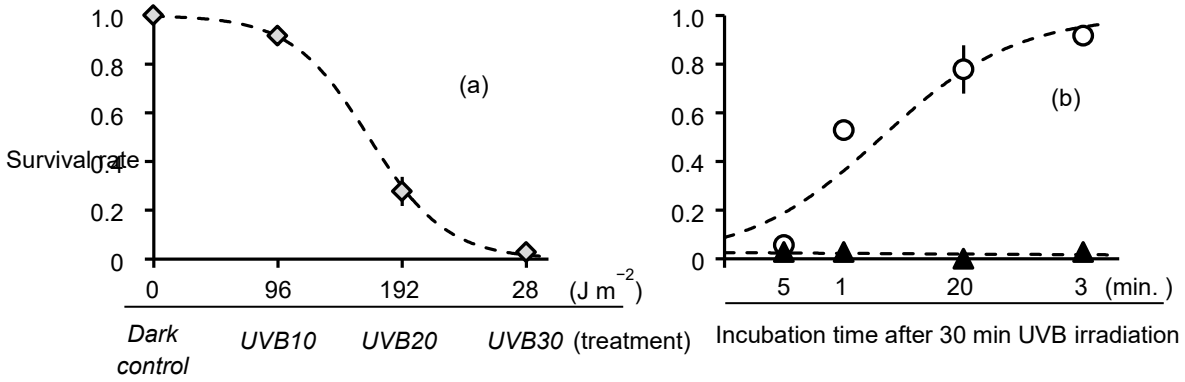

Fig. 14. (a) Mean survival rate of *T. urticae* larvae exposed to each irradiation treatment (dark control [UVB dose: 0 J m^{-2}], UVB10 [96 J m^{-2}], UVB20 [192 J m^{-2}] and UVB30 [288 J m^{-2}]) in experiments of DNA damage detection in UVB-irradiated larvae. Dashed lines represent the estimated GLM. Vertical bars represent standard error (SE).
(b) Mean survival rate of *T. urticae* larvae exposed to each irradiation treatment (±PR5, 10, 20 and 30) in experiment of DNA damage repair in photoreactivaiton treatment. Open circles represent +PR treatment. Closed triangles represent −PR treatment. Dashed lines represent the estimated GLMM. Vertical bars represent the 95% CI range.

DNA damage repair in photoreactivation treatment.

After UVB irradiation, surviving individuals recovered over time under +PR treatment. After 30 min VIS irradiation, almost all individuals developed normally into adults. Under dark conditions (−PR treatment), all individuals died without recovery. The relationship between irradiation treatment and time course significantly affected

survival (GLMM, +PR, $P = 0.27899$; time course, $P = 0.82014$; interaction (+PR × time course), $P = 0.00502$; Fig. 14b).

After UVB irradiation, the remaining CPD decreased gradually with incubation time under VIS irradiation treatment. In contrast, under dark conditions, CPD decreased rapidly after 5 min of incubation and subsequently increased with incubation time. The GLMM analysis revealed that the interaction of VIS irradiation and incubation time significantly affected CPD variation (Table 4; Fig. 15C). The 6-4PP levels varied in a similar manner to CPD but were not significant (Table 4; Fig. 15D).

Table 4. Results of fixed effect in GLMM analysis of the CPD/6-4PP remaining percentage [remaining CPD/6-4PP percentage ~ ±PR × time course + random effect (family = Gaussian)].

	Coefficient	SE	df	t-statistic	Pr(>|t|)
CPD					
(Intercept)	62.4177	12.395	13.027	5.036	2.27×10^{-4}
+PR treatment (A)	22.4701	15.9222	24.003	1.411	0.17
time course (B)	0.4875	0.6669	24.003	0.731	0.47
A × B	−3.1327	0.9432	24.003	−3.332	0.0028
6-4PP					
(Intercept)	0.707953	0.167362	10.84	4.23	0.0015
+PR treatment (A)	0.297145	0.204413	20.906	1.454	0.16
time course (B)	0.003452	0.009244	21.006	0.373	0.71
A × B	−0.020623	0.013001	21.212	−1.586	0.13

- Discussion

DNA bases can be divided into two groups based on their structure: purine and pyrimidine bases. When DNA is exposed to UV radiation, two adjacent pyrimidine bases are linked together by the high UV energy, producing CPD and 6-4PP. Approximately 75% and 25% of UVB-induced DNA lesions are CPDs and 6-4PPs, respectively (Mitchell and Nairn 1989). CPD is thought to be the most cytotoxic because of its abundance. On the other hand, because of the formation of DNA bends, 6-4PPs may cause more serious lethal effects on organisms (Sinha and Häder 2002). These abnormal structures block transcription and replication of DNA, inducing mutation and death.

The UVB dose-dependent increases in CPD and 6-4PP frequencies and mortality support that the formation of DNA lesions is a major factor in the biological impact of UVB irradiation in *T. urticae*. CPD and 6-4PP formation by UVB irradiation were demonstrated in aquatic plankton, plants and cultured cells (Yasuhira et al. 1991;

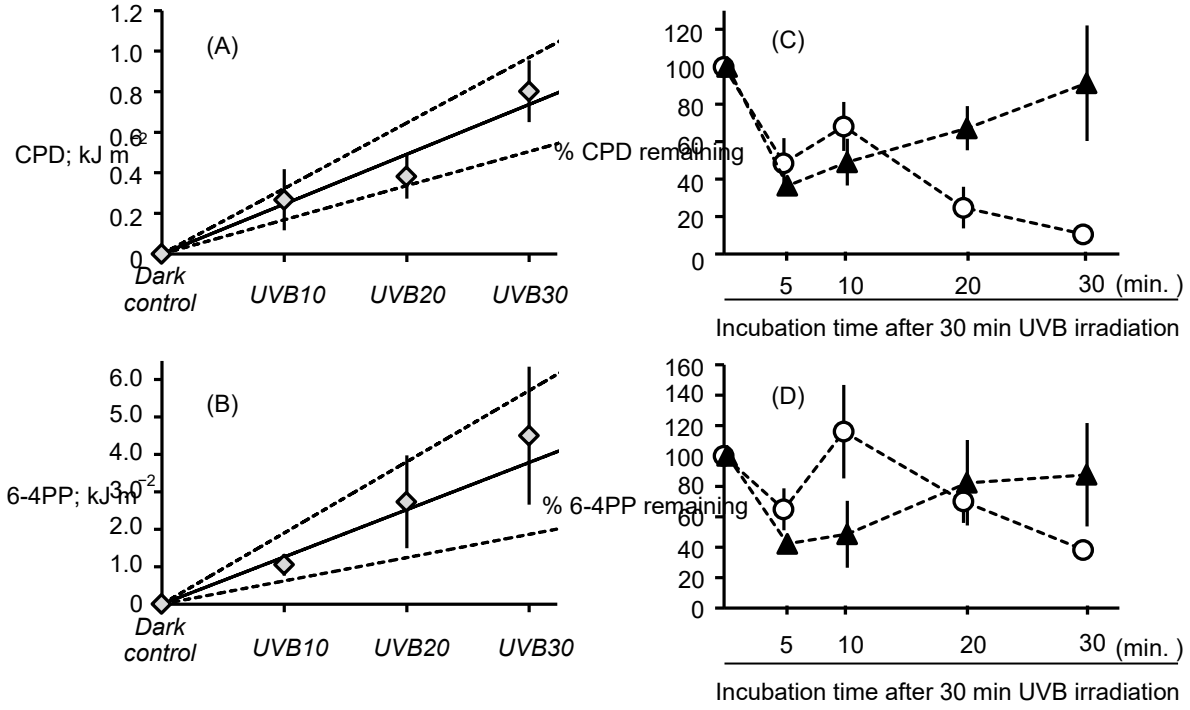

Fig. 15. Left: (A) UV-induced CPD frequencies in *T. urticae* larvae just after exposure to UVB irradiation treatment (dark control, UVB10, UVB20 and UVB30). Solid line represents the linear regression between CPD frequency and UVB dose, dotted lines the 95% confidence interval (CI), and vertical bars the SE. (B) UV-induced 6-4PP frequencies in *T. urticae* larvae just after exposure to UVB irradiation treatment (dark control, UVB10, UVB20 and UVB30). Solid line represents the linear regression between 6-4PP frequency and UVB dose, dotted lines the 95% confidence CI, and vertical bars the SE. The vertical axis represents the UVC dose level equivalent to CPD/6-4PP frequency in sample DNA.

Right: Percentage of remaining (C) CPD and (D) 6-4PP based on DNA damage frequencies in the UVB30 treatment samples at each incubation time point after 30 min of UVB irradiation. Open circles represent incubation with VIS light irradiation (+PR). Closed triangles represent no VIS light irradiation (−PR). Vertical bars represent the SE range.

Mitchell et al. 1993; Mitani et al. 1996; Malloy et al. 1997; Hidema et al. 2000; Li et al. 2002; Macfadyen et al. 2004; Connelly et al. 2009; Reef et al. 2009). These reports also demonstrated the lethal effects caused by UV-induced DNA lesions. *T. urticae* larvae exposed to UVB radiation appeared normal and healthy until they entered the developmental stage of protochrysalis. Many failed to moult or did not survive after moulting, as was observed in our previous study (Murata and Osakabe 2014). The chrysalis-specific mortality suggested that genes essential for ecdysis and morphosis were affected by the formation of CPDs and 6-4PPs.

When *T. urticae* eggs were exposed to UVB radiation within 24 h after oviposition, the photoreactivation efficiency decreased with the increase in time lag between UVB

irradiation and VIS irradiation, and no reactivation effects were observed when the time lag reached 4 h (Murata and Osakabe 2014). In eggs 24–48 h after oviposition, the larval body is formed, based on the germinal disk (Dearden et al. 2002), and this is the stage most vulnerable to UVB radiation. I think that if UVB-induced DNA lesions are repaired before the initiation of gene expression in the egg and protochrysalis for morphosis and ecdysis, the mites can survive the biological impacts of UVB radiation.

The correspondence between an increasing pattern of survivorship and a reduction in CPDs by VIS irradiation indicates that PER of CPDs is a major factor in the remarkable photoreactivation of *T. urticae* larvae exposed to UVB irradiation.

In contrast, 6-4PP decreased little after VIS irradiation 30 min after UVB irradiation in both −PR and +PR treatment. Thus, I additionally investigated 6-4PP frequencies 1 day after irradiation treatment. Mites exposed to UVB, followed or not followed by VIS irradiation, were kept under dark conditions until 6-4PP analysis.

I found no 6-4PPs in the genomic DNA after either treatment (data not shown). The difference in the remaining ratios between CPDs and 6-4PPs was compatible with the fact that *T. urticae* possesses CPD photolyase genes, but no (6-4) photolyase genes (Grbić et al. 2011). Actually, (6-4) photolyase gene has been identified only in limited organisms such as *Drosophila* (Todo et al. 1996; Sinha and Häder 2002; Weber 2005). 6-4PPs may be repaired by other repair mechanisms, such as NER, that might operate at a slower rate than PER (Thoma 1999; Kienzler et al. 2013).

In several fishes, NER is robust, and 50% of CPDs are repaired in the dark within 9 h; PER is co-dependent on NER (Mitchell et al. 2009; Kienzler et al. 2013). In contrast, ≈90% of CPDs were repaired after 30 min of irradiation by VIS in this study. Less reduction in CPDs was observed in mites kept in the dark. Therefore, most CPDs are probably repaired by CPD photolyases in *T. urticae*.

Since I employed a comparative measurement method to quantify DNA lesions, I could not compare the frequencies of CPDs with 6-4PPs directly in our data. Increasing survivorship by irradiation with VIS after exposure to UVB radiation was compatible with decreasing CPD frequencies. Moreover, CPDs generally comprise the majority (≈75%) of UV-induced DNA lesions (Sinha and Häder 2002; Rastogi et al. 2010). PER for CPDs may be a major repair pathway for UVB-induced DNA lesions and essential for the survival of *T. urticae* under ambient UVB radiation. However, there remains unexplainable trend in result about decreasing of CPDs and 6-4PPs, which were rapid decreasing at 5 min incubation and following increase under dark condition. Including these obscurities, there is still room to verify this repair.

Section2: Gene Expression Analysis about UVB Irradiation and Photoreactivaitgon in Larva

- Materials and Methods

Gene expression analysis in UVB-irradiated larvae.

T. urticae larvae on leaf disks and polyester film in four Petri dishes were prepared as outlined in damage detection and assigned to UVB10, UVB20 or UVB30 treatment or the dark control. Immediately after the irradiation treatments, total RNA was extracted. Larvae on the film were homogenised using a pellet mixer in 800 µl ISOGEN (Nippon Gene Co., Ltd.) in a 1.5-mL micro tube (Eppendorf) and treated following the manufacturer's instructions. The resulting RNA pellet was dissolved in 10 µl nuclease-free water (Qiagen). The quantities and qualities of the RNA samples were evaluated using a spectrophotometer and by 1% agarose gel electrophoresis. Each series of treatments was performed in three replicates.cDNA was synthesised from total RNA samples by reverse transcription using ReverTra Ace® qPCR RT Master Mix with gDNA Remover (Toyobo Co., Ltd. Life Science Department). Synthesised cDNA samples were diluted 30-fold in nuclease-free water and applied to quantitative real-time PCR (qPCR) analysis.

T. urticae has four copies of the CPD photolyase gene (*tetur12g04440*, *tetur12g04460*, *tetur35g00010* and *tetur35g00030*), all of which are highly homologous to each other. Particularly, *tetur12g04440*, *12g04460*, and *35g00010* have almost same sequences with some single nucleotide differences. Therefore, I designed a universal primer set for three CPD photolyase genes other than the *tetur35g00030* gene to check the expression pattern of total three copies (*tetur12g04440*, *tetur12g04460*, and *tetur35g00010*) (Table 5). I also designed a primer set for the XPA gene, which is present as a single copy (*tetur05g03450*) (Table 5). The expression patterns of total three copies of CPD photolyase genes and XPA gene were evaluated by means of qPCR with intercalator method using two housekeeping genes: glyceraldehyde 3-phosphate dehydrogenase (GAPDH; a single copy; *tetur25g00250*) gene and three copies of Elogation factor 1 alpha (EF-1α; three copies; *tetur08g02980*, *tetur08g03040*, and *tetur08g03070*) as reference genes. These housekeeping genes were previously revealed to be suitable as a reference gene to compare expression patterns in UV-irradiated spider mites (Niu et al. 2012), and I confirmed that the result of expression pattern was same regardless of either reference gene. Real-time PCR primers were designed using the primer3plus software (Untergasser et al. 2007;

http://www.bioinformatics.nl/cgi-bin/primer3plus/primer3plus.cgi/) and GENETYX Ver. 9 GENETIC INFORMATION PROCESSING SOFTWARE (GENETYX Co., Ltd.), based on the *T. urticae* gene annotation file (Sterck et al. 2012; ORCAE: http://bioinformatics.psb.ugent.be/orcae/overview/Tetur; Table 5). The specificity of the primer set against each gene was checked by BLAST search and the electrophoresis of RT-PCR product.

On the other hand, the remaining CPD photolyase gene (*tetur35g00030*) was revealed only 365 nucleotides, including the intron, and its coding sequence is only 108, which also has high homology with others. Therefore, to evaluate the expression of *tetur35g00030*, qPCR with cycling probe PCR assay for single nucleotide polymorphism (SNP) genotyping, which detect specific PCR product by fluorescence of DNA-RNA-DNA chimera probe breaking by detecting the single nucleotide specificity (Bekkaoui et al. 1996; Modrusan et al. 1998; Itabashi et al. 2010), was applied. When the probe hybridizes to its complementary target DNA, the probe is cleaved by RNase H at RNA linkage, which covers specific nucleotide point, and emits fluorescence. I used GAPDH as reference gene. The cycling probe-primer sets were designed using a free software, "CycleavePCR® Assay Designer" supported by TaKaRa bio Inc. (https://www.takara-bio.co.jp/cycleave_design/cycleave_designer_snps_index.php; Table 6).

The qPCR with intercalator method was carried out using THUNDERBIRD® SYBR® qPCR Mix (TOYOBO Co., Ltd. Life Science Department) in a final reaction mixture volume of 10 µl with 5 µl THUNDERBIRD® SYBR® qPCR Mix, 0.5 µl each primer (10 pmol/ µl), 3 µl cDNA template and 1 µl nuclease-free water. The reactions were performed in a Bio-Rad iQ2 thermocycler (Bio-Rad Laboratories, Inc.) under the following conditions: initial denaturation at 95°C for 3 min, followed by 40 cycles at 95°C for 15 s and 60°C for 45 s, and elongation at 60°C for 10 s. Finally, melt curve analyses (60–95°C) were included at the end to confirm the consistency of the amplified products.

Cycleave®PCR Reaction Mix (TaKaRa bio Inc.) was used for the cycling probe PCR assay for single nucleotide polymorphism (SNP) genotyping. A reaction mixture for qPCR (20 µl) was composed of 10 µl Cycleave®PCR Reaction Mix, 0.4 µl each primer (10 pmol/ µl), 0.8 µl cycleave chimera probe (5 pmol/ µl), 2 µl cDNA template and 6.4 µl nuclease-free water. The reactions were performed in a LightCycler nano (Roche Diagnostics, Inc.) under the following conditions: initial denaturation at 95°C for 30 s, followed by 45 cycles at 95°C for 10 s and 60°C for 30 s.

Relative expression was calculated using the $2^{-\Delta\Delta Ct}$ method (Livak and Schmittgen

2001). Two technical replicates were performed for each of three biological replicates. In advance, using different cDNA dilution, ΔCt values were plotted against each cDNA concentration to confirm the amplification efficiency equivalent between target and reference gene. The housekeeping genes which showed less variation in Ct values among samples were selected and the obtained Ct values of the gene were used for calculation of ΔCt values. To evaluate the effect of UVB on CPD photolyase and XPA gene expression, the effects of irradiation treatment on the ΔΔCt values were evaluated using GLM (Gaussian) analysis in R.

After irradiation treatment and RNA sample collection, 12 larvae on each leaf disk were maintained in a dark chamber (25°C, 0 L:24 D) and observed until all individuals died or progressed to adulthood. To evaluate the effect of UVB dose on the survival rate, GLM (Binomial) analysis was performed using the "glm" module in R.

Table 5. Primer sequences used for quantitative real-time RT-PCR (intercalator method).

Genes	Primer sequences (5' to 3')	Product length (bp)
CPD Photolyase (*tetur12g04440*, *tetur12g04460*, and *tetur35g00010*)	F: TGCAATTGGTTCGCGATG R: GCGATTTCCAGTGCTTCTTC	103
XPA (*tetur05g03450*)	F: TTGGCTCGTGGTGATATGAGAC R: AAGGCTTCCTCAGATTCCCAAAC	83
GAPDH (*tetur25g00250*)	F: TGGAAAACTCACCGGTATGG R: CACTTTCTGAAGCAGCCTTG	131
EF 1-α (*tetur08g02980*, *tetur08g03040*, and *tetur08g03070*)	F: CCAAGTAAGCCAATGTGTGTTG R: GCAACAGTTTGTCGCATATCAC	86

Table 6. Primer and probe sequences used for quantitative real-time RT-PCR (cycling probe method). In the probe, small letter represents the single nucleotide difference to cleave DNA-RNA-DNA chimera probe by RNase H and detect the specific PCR product by emitting florescent.

		Sequences (5' to 3')	Product length (bp)	Fluorescence
CPD Photolyase (*tetur35g00030*)	Primer F	TGGAGAGAGAGATTTATGG	131	HEX
	Primer R	TTGGGTCTGATAGTTCG		
	Probe	GGAATTtGCT		
GAPDH (*tetur25g00250*)	Primer F	AGCCTTAGCTGCACCAGTAG	194	FAM
	Primer R	GTACAACCAACTGTCTTGCTC		
	Probe	ATgAGACCTTC		

Gene expression analysis in photoreactivation treatment.

T. urticae larvae on leaf disks and polyester film in eight Petri dishes were prepared as described above, and all dishes were exposed to UVB irradiation for 30 min. Then,

four Petri dishes were assigned to +PR5, +PR10, +PR20 or +PR30 treatments, and the remaining four dishes were assigned to −PR5, −PR10, −PR20 or −PR30 treatments. These continuous irradiation treatments were conducted on the same day. After irradiation treatment, RNA extraction and gene expression analysis were performed using the same procedures as in gene expression analysis in UVB-irradiated larvae. Each series of treatments was performed in three replicates.

To evaluate the effects of VIS irradiation and time course after UVB irradiation on CPD photolyase and XPA gene expression, the GLMM, in which repeated data have random effects, was constructed using the “lmer” module in the “lme4” and “lmerTest” package in R.

After irradiation treatment and RNA sample collection, 12 larvae on leaf disks were kept in a dark chamber (25°C, 0 L:24 D) and observed until all individuals died or progressed to adulthood. To evaluate the effect of VIS irradiation and the time course after UVB irradiation on survival rate, the GLMM, in which repeated data have random effects, was constructed using the “glmer” module in the “lme4” package in R.

- Results

Gene expression analysis in UVB-irradiated larvae.

The survival rate decreased as the UVB cumulative dose increased (GLM, $P = 2.69 \times 10^{-8}$). Similar to the results in DNA damage detection, most individuals died at the protochrysalis stage.

The expression level of the CPD photolyase gene, both total three gene expression (*tetur12g04440*, *tetur12g04460*, and *tetur35g00010*) and one specific gene expression (*tetur35g00030*) were slightly increased by UVB irradiation, although no significant effects were detected (Table 7, Fig. 16A, 16B).The expression level of the XPA gene was significantly increased by UVB irradiation (Table 7; Fig. 16C).

Gene expression analysis in photoreactivation treatment.

After UVB irradiation, survivors recovered over time with +PR treatment. After 30 min VIS irradiation, nearly all individuals developed normally into adults. Under dark conditions (−PR treatment), all individuals failed to recover and died. The relationship between irradiation treatment and the time course significantly affected survival (GLMM; +PR, $P = 0.252091$; time course, $P = 0.566516$; interaction (+PR × time course), $P = 0.004095$).

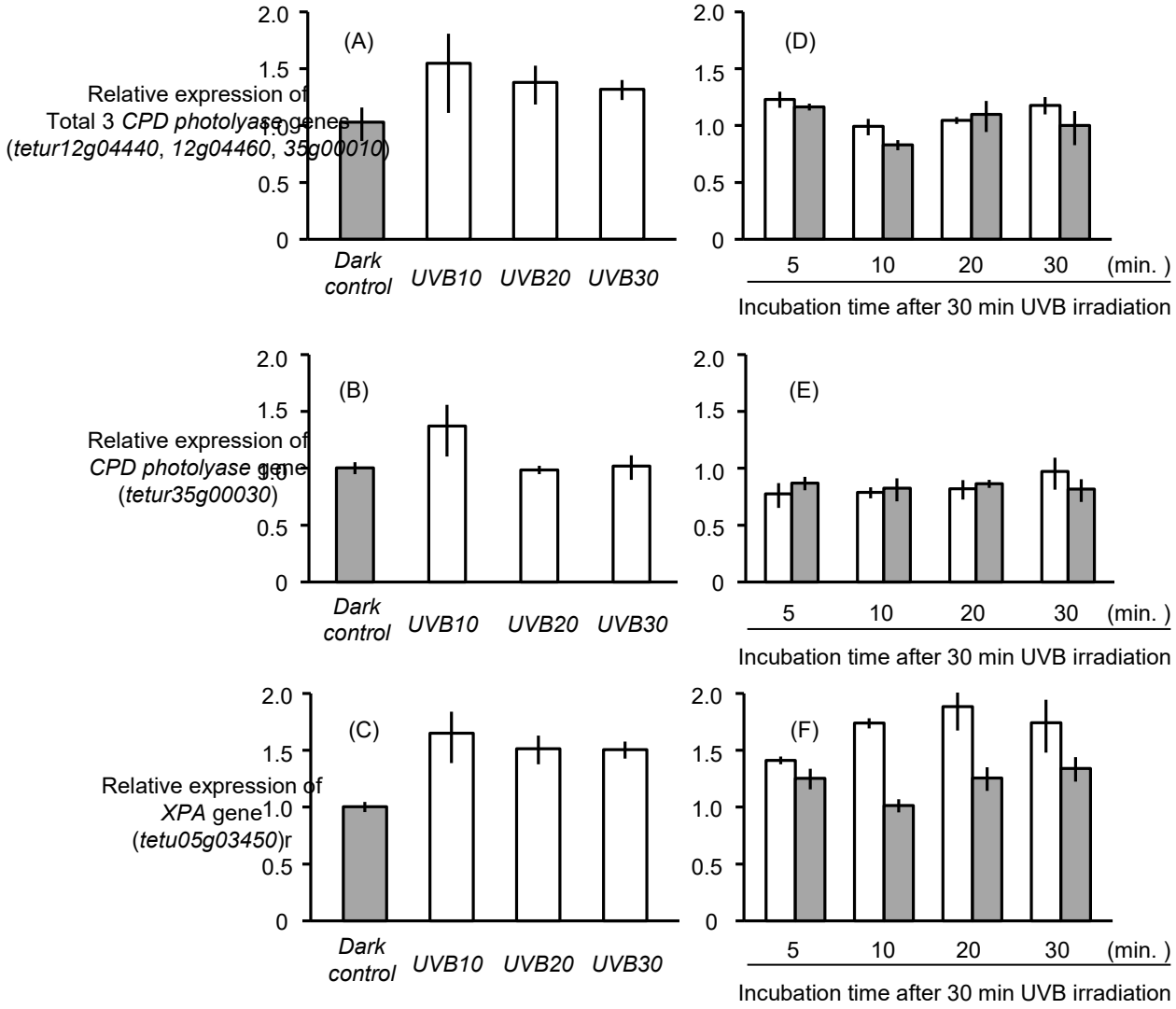

Fig. 16. Left: (A) The expression levels of the total 3 CPD photolyase gene (*tetur12g04440*, *tetur12g04460*, and *tetur35g00010*) evaluated by intercalator method in *T. urticae* larvae. (B) The expression levels of the other CPD photolyase gene (*tetur35g00030*) evaluated by cycling probe method in *T. urticae* larvae. (C) The expression levels of the XPA gene evaluated by intercalator method in *T. urticae* larvae. The relative expression was calculated based on the value of the "dark control" expression, which was assigned an arbitrary value of 1. GAPDH was used as the reference gene. Vertical bars represent the SE range.
Right: The expression levels of (D) total 3 CPD photolyase (*tetur12g04440*, *tetur12g04460*, and *tetur35g00010*), (E) the other CPD photolyase (*tetur35g00030*) and (F) the XPA gene in *T. urticae* larvae at each incubation time point after 30 min of UVB irradiation. The expression levels were evaluated by intercalator method in (D) total 3CPD photolyase and (F) XPA genes, and cycleave probe method in (E) the other CPD photolyase gene, respectively. The relative expression was calculated based on the value of the "dark control" expression, which was assigned an arbitrary value of 1. GAPDH was used as the reference gene. Open bars represent incubation with VIS light irradiation (+PR). Grey bars represent no VIS light irradiation (−PR). Vertical bars represent the SE range.

After UVB irradiation, CPD photolyase gene expression levels, both total three gene expression (*tetur12g04440*, *tetur12g04460*, and *tetur35g00010*) and one specific gene expression (*tetur35g00030*) did not varied, regardless of whether VIS irradiated and incubation length (Table 8; Fig. 16D, 16E). For the XPA gene, expression levels were significantly up-regulated by exposure to VIS irradiation after UVB irradiation, but they did not change under dark conditions (Table 8; Fig. 16F).

Table 7. GLM analysis of the effects of UVB irradiation on total 3 CPD photolyase (*tetur12g04440*, *tetur12g04460*, and *tetur35g00010*), the other CPD photolyase (*tetur35g00030*) and XPA (*tetur05g03450*) gene expression [ΔΔCt ~ irradiation treatment (family = Gaussian)].

	Coefficient	SE	t-statistic	Pr(>|t|)
Total 3 CPD photolyase				
(Intercept)	6.494×10^{-19}	0.2807	0	1
UVB10	−0.5043	0.397	−1.270	0.24
UVB20	−0.4279	0.397	−1.078	0.31
UVB30	−0.3890	0.397	−0.980	0.36
The other CPD photolyase				
(Intercept)	8.012×10^{-17}	0.1887	0	1
UVB10	−0.3914	0.2668	−1.467	0.18
UVB20	0.02316	0.2668	0.087	0.93
UVB30	-1.718×10^{-4}	0.2668	−0.001	1
XPA				
(Intercept)	1.071×10^{-16}	0.1564	0	1
UVB10	−0.6764	0.2212	−3.058	0.016
UVB20	−0.5827	0.2212	−2.634	0.030
UVB30	−0.5849	0.2212	−2.645	0.030

- Discussion

Photolyase gene expression responses to photoreactivation vary among organisms. In yeast, transcription of photolyase was enhanced by exposure to 254 nm light (Sebastian et al. 1990). A photolyase gene expressed in *Trichoderma harzianum*, a common soil fungus, was induced within 30 min by blue light without UVB irradiation (Berrocal-Tito et al. 1999). In contrast, transcription of photolyase increased more than 10-fold 4–8 hours after UVC (254 nm wavelength) and VIS irradiation in cultured cells from goldfish *Carassius auratus* (Yasuhira and Yasui 1992).

In *T. urticae*, CPD photolyase gene expression was slightly induced by UVB irradiation. In our verification, total expression of three CPD photolyase genes (*tetur12g04440*, *tetur12g04460*, and *tetur35g00010*) were analysed all together.

Although I acknowledge a possibility that expression pattern vary among genes, it seems that total expression of all four genes (*tetur12g04440*, *tetur12g04460*, *tetur35g00010*, and *tetur35g00030*) was similarly induced little by UVB irradiation because similar expression pattern was also observed in solely analysed *tetur35g00030*. VIS irradiation after UVB irradiation did not induce CPD gene expressions.

Eventually, CPD photolyase gene expression was not changed significantly, even though 100% lethal level of UVB and 100% recovery level of VIS irradiation treatment. In the field, they generally have the risk that they might be exposed to ambient solar UVB radiation. Hence, it is likely that CPD photolyase gene is constitutively expressed. Including this possibility, this gene expression mechanism which is concerned with PER function is worth investigating in further detail in *T. urticae*.

Table 8. Results of fixed effect in GLMM analysis of the total 3 CPD photolyase (*tetur12g04440*, *tetur12g04460*, and *tetur35g00010*), the other CPD photolyase (*tetur35g00030*) and XPA (*tetur05g03450*) gene expression [ΔΔCt ~ ±PR × time course + random effect (family = Gaussian)].

	Coefficient	SE	df	t-statistic	Pr(>|t|)
Total 3 CPD photolyase					
(Intercept)	−0.043137	0.164588	18.792	−0.262	0.80
+PR treatment (A)	−0.086608	0.226439	18	−0.382	0.71
time course (B)	0.002796	0.008483	18	0.33	0.75
A × B	−0.003398	0.011997	18	−0.283	0.78
The other CPD photolyase					
(Intercept)	0.225407	0.187087	3.688	1.205	0.30
+PR treatment (A)	0.261277	0.147090	18	1.776	0.093
time course (B)	0.002473	0.005510	18	0.449	0.66
A × B	−0.014589	0.007793	18	−1.872	0.078
XPA					
(Intercept)	−0.122450	0.15355	8.092	−0.797	0.45
+PR treatment (A)	−0.470510	0.170398	18	−2.761	0.013
time course (B)	−0.008590	0.006384	18	−1.346	0.20
A × B	−0.000237	0.009028	18	−0.026	0.98

Contrary to our expectation, the XPA gene associated with NER was upregulated by UVB irradiation followed by VIS irradiation, rather than the CPD photolyase genes. XPA binds damaged DNA and makes DNA open complex in the NER process (Batty and Wood 2000). In contrast to our data, recent expression pattern analysis of the intertidal copepod, *Tigriopus japonicas*, revealed up-regulation of genes associated with DNA repair, such as base excision repair (BER) and mismatch repair, but down-regulation of NER-related genes, including XPA, in response to UVB radiation

(Rhee et al. 2012). Increases in BER-related gene expression and heat shock protein after UVB irradiation were also reported in the cycloid copepod, *Paracyclopina nana* (Won et al. 2015). NER is a complicated DNA repair process that involves many genes, and studies of its mechanisms are currently underway in many organisms (Rastogi et al. 2010; Budden and Bowen 2013; Kienzler et al. 2013; Karentz 2015). Because DNA lesions are produced by a variety of environmental stressors, such as reactive oxygen species, chemicals and others (Mitani and Shima 1995; Ahmed et al. 2011; Speidel 2015), DNA repair genes possibly respond to various environmental stimuli. In order to reveal these expression mechanisms, it is necessary to obtain more information about NER- and PER-associated gene expression.

Chapter6: Chrysalis Phase-specific Mortality in UVB-irradiated *T. urticae* Larvae

About the effect of UVB radiation, the phase-specific mortality is observed in *T.urticae* eggs and larvae (Murata and Osakabe 2014). The UVB vulnerability of eggs was varied during embryogenesis development. Eggs aged 24–48 h after oviposition were the most vulnerable to UVB, which these phase is consist with the timing of significant formation of germinal disk (Dearden et al. 2002). In the case of larvae, the individuals exposed to UVB radiation seemed phenotypically normal. However, when they developed to the next protochrysalis stage, UVB-induced death eminently occurred. Many individuals fault moulting and trapped in old epidermis, or stop development and shrinking. Phase of the formation of germinal disk during embryogenesis and chrysalis stage are assumed dynamic physiological changes about body formation of next developmental stage.

UVB-induced abnormal DNA structures, DNA damages, CPD and 6-4PP inhibit the transcription and replication of DNA (Sinha and Häder 2002). Also in *T. urticae* larvae, CPD and 6-4PP were confirmed previously (Murata and Osakabe in press). During dynamic differentiation in embryogenesis and chrysalis, many gene expressions and DNA replications were expected. Therefore, I hypothesized that DNA damages generated by UVB irradiation at larval stage disarranged transcriptions and replications essential for physiological change during chrysalis stage. Whereas the lethal effect of UVB for arthropods has been well reported (Wübben 2000; Connelly et al. 2009; Murata and Osakabe 2013; Tachi and Osakabe 2012), the developmental phase-specific death is never reported. The information about this characteristic mortality can contribute to clarify physiological mechanism of UVB effect.

In this chapter, I conducted the observation of larvae exposed to high lethal level of UVB and proved the protochrysalis phase-specific death. Furthermore, the whole transcriptomes were profiled between protochrysalis individual exposed/non-exposed to UVB radiation at their larval stage to clarify the differentially expressed genes and get the trigger of mechanism causing phase-specific mortality.

Chapter 6

Section1: Verification of UVB-induced Developmental Phase-specific Mortality

- Materials and Methods

A kidney bean leaf disk (5.0 × 5.0 cm) was placed on water-soaked cotton in each of 16 Petri dishes. Twenty adult *T. urticae* females were introduced on each leaf disk. They were kept under 25 °C, 16L: 8D condition for 24h. After 24h, females were removed and Petri dishes were covered with lids to keep high humidity inside. It was already revealed that this treatment can delay and adjust the timing of egg hatching. Four days after this treatment, lids were opened to make humidity low and induce egg hatching (Ubara and Osakabe 2015). After 3 hours, hatched larvae on 8 Petri dishes were irradiated by UVB lamp (0.58 W m^{-2}) for 1 hour ("+UVB" treatment) and cumulative irradiance was 2.088 kJ m^{-2}, which irradiance was ~100% lethal level for *T. urticae* larvae in verification in Chapter3. During irradiation, the other Petri dishes were placed on shelf outside of UV-opaque film ("−UVB" control). In advance, about 40 kidney bean leaf disks (1.0 × 1.0 cm) were placed on water-soaked cotton in each of 2 rectangle plastic cases. After irradiation treatment, randomly selected ~40 larvae in +UVB and −UVB treatment were introduced onto leaf disks in each rectangle plastic cases, respectively (one larva per leaf disk). Larvae in plastic cases were kept in the chamber (25 °C, 16L:8D) and survivals and developmental stages were observed every day until all individuals developed to adult or died. Each series of treatment was performed with three replicates.

To evaluate the effect of UVB irradiation, their last survivals were compared between +UVB and –UVB treatment using Fisher's exact test. In addition, using Kaplan-Meier method, the attainment rate to protochrysalis was compared between +UVB and −UVB treatment. Furthermore, dead individuals in +UVB treatment were categorized into the developmental phase when they died and phase-specific mortality was evaluated by one-way ANOVA and Tukey-Klumer method.

- Results

Almost all the larvae died on +UVB, whereas all individuals normally developed to adulthood on –UVB treatment (Fig. 17; Fisher's exact test: $P < 2.2\times10^{-16}$). Over 80% individuals developed to protochrysalis 1 day after treatment in –UVB control. On the other hand, the developmental rate significantly delayed in +UVB treatment (Fig. 18;

log-rank test: $P < 0.001$), all individuals still remained in larval phase on that day. After 2days, ~20% individuals developed to protochrysalis and then, most individuals gradually developed. At last, ~80% developed to protochrysalis over 9days. All these protochrysalis ultimately died by developmental stop or failure to moult. The other ~20% individuals never developed to protochrysalis. They seemed normally until 1 day after irradiation. However, larvae had writhed after 2 days of irradiation and gradually died at and after 15th days (Fig. 18).

All individuals died in developmental phases of larvae, protochrysalis, or protonymph. In particular, almost individuals died on protochrysalis by developmental stop (Fig. 19, 20; one-way ANOVA: P = 0.000549, Tukey's HSD, $P < 0.01$), which was consistent with the results in previous chapters.

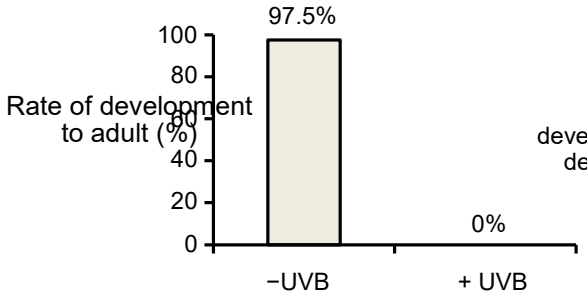

Fig. 17. Developmental rate of *T. urticae* larvae after exposure to UVB radiation. "+UVB" represent the survivals irradiated with UVB (0.58 W m^{-2}) for 1 hour. "−UVB" represent that put out of UV-cut film (0 W m^{-2}) during UVB exposure.

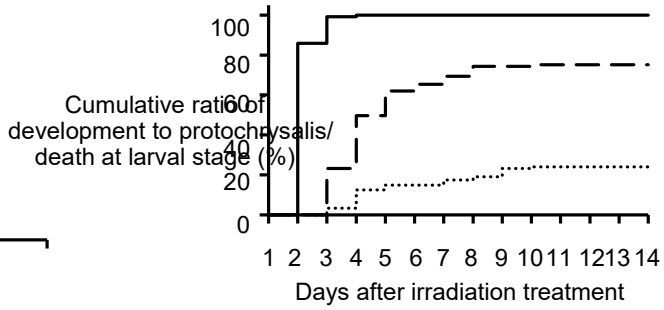

Fig. 18. Kaplan Meier curves of cumulative developmental rate to protochrysalis in "−UVB" (solid line) and "+UVB" (dashed line). Dotted line represents the cumulative dead rate at larval stage in "+UVB" treatment.

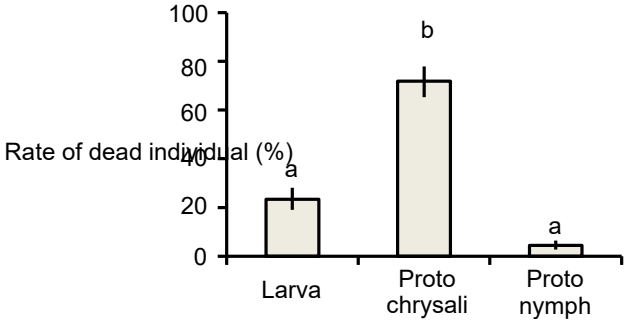

Fig. 19. Rate of dead individuals at each developmental stage in "+UVB" treatment. Small letters represent the significant difference among developmental stage.

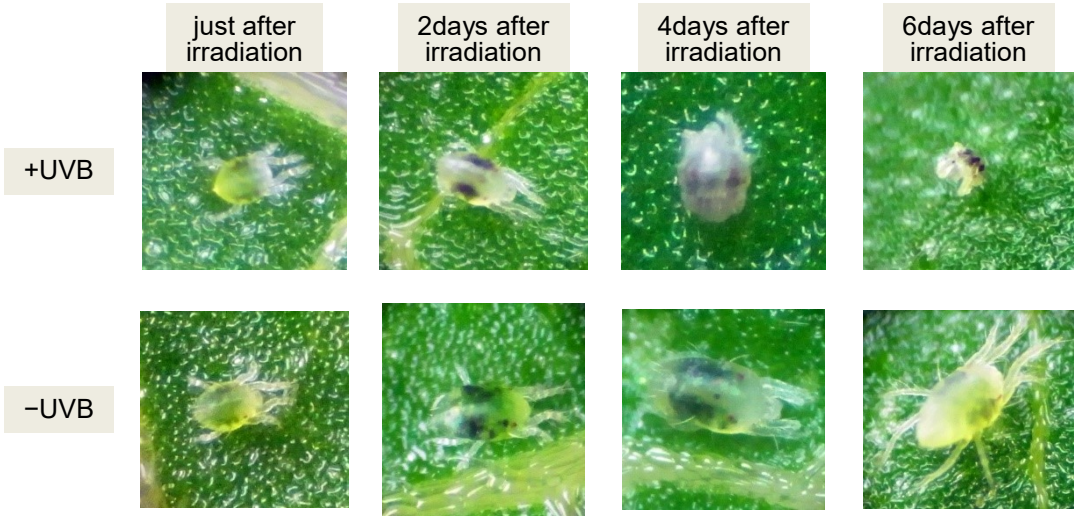

Fig. 20. Comparison of phenotypes between +UVB treatment and –UVB control which were just after, 2days, 4days, and 6days after irradiation treatment.

- Discussion

The mortalities induced by UVB radiation were reported in many organisms (Hanawalt 1966; Kouwenberg et al. 1999b; Zagarese et al. 1997; Sakai et al. 2012). However, the UVB-induced developmental stage-specific death has never been reported in metazoan. The larvae irradiated by UVB lamp died not in the larval phase but the protochrysalis. Therefore, the lethal effect of UVB seemed to become apparent at the specific developmental phase.

UVB radiation has various effects inducing death and developmental delay for spider mites (Suzuki et al. 2009; Murata and Osakabe 2013). One of the main causes of them is thought to be a DNA damages, CPD and 6-4PP. These abnormal structures block transcription and replication of DNA (Sinha and Häder 2002). In *T. urticae*, these DNA damages were induced by exposure to UVB, with increasing of the mortality (Section1 of Chapter5). In relation between formation of DNA damages and protochrysalis phase-specific death induced by UVB, I hypothesized that CPD and 6-4PP inhibit the certain gene expressions which are essential for development, metamorphosis, and moulting, thus inducing protochrysalis phase-specific mortality. In order to verify this hypothesis and explore the causes of this phenomenon, in the next section, I compared the whole transcriptome profiles and clarified the differentially expressed genes,

between protochrysalis individuals exposed/non-exposed to UVB radiation at their larval stage.

Section2: Whole Transcriptome Analysis on Protochrysalis between UVB Irradiated and Non-irradiated Treatments

- Materials and Methods

Preparation of *T. urticae* larvae and UVB irradiation treatment were taken using same experimental procedure as the verification of UVB-induced developmental phase-specific mortality. After irradiation treatment, they were kept in chamber. A large number of individuals developed into protochrysalis 1day after UVB irradiation in –UVB treatment and 2days after UVB irradiation in +UVB treatment. More than 100 chrysalises in each treatment were sampled into 1.5 ml-micro tube using fine brush, and homogenized in 800 μl ISOGEN using pellet mixer. Each homogenate was treated following the manufacturer's instructions. The resulting RNA pellet was dissolved in 80 μl nuclease-free water (Qiagen). The quality and quantity of the RNA samples were evaluated using a spectrophotometer. Each series of treatments was sampled with three replicates.

The RNA samples were used for transcriptome sequencing and characterization. The transcriptomes were compared between +UVB and –UVB treatment using RNA sequenced reads. RNA read sequence and transcriptome analysis were commissioned to Macrogen Inc. The experimental procedures followed Martin and Wang (2011). Briefly, in isolated total RNA, DNA contamination was eliminated using DNase. After mRNA purification, the purified RNA was randomly fragmented for short read sequencing. These fragmented RNA was reverse-transcribed into cDNA and adaptors were ligated both ends of these fragments. After amplifying fragments using PCR, fragments with insert sizes between 200–400 bp were selected for paired-end sequencing; both ends of the cDNA were sequenced by the 100 bp read length. After removal of artifacts in order to reduce biases in analysis, trimed reads are mapped to *T. urticae* reference genome (NCBI *Tetranychus urticae* Annotation Release 100; NCBI GCF_000239435.1) with TopHat, splice-aware aligner. Transcript is assembled by Cufflinks with aligned reads that contain paired-end information. The expression profiles of assembled transcripts for each sample are calculated by Cufflinks. Expression profiles are represented as normalization value which is based on transcript length and depth of coverage. The

FPKM (Fragments Per Kilobase of transcript per Million Mapped reads) value was used as expression profile. In different irradiation treatment groups, genes or transcripts that express differentially are filtered out through statistical hypothesis testing (|fold change| ≥2 & Independent t-test raw p-value<0.05). In case of known gene annotation, functional annotation and gene-set enrichment analysis are performed using GO and KEGG database on differentially expressed genes.

- Results

RNA-sequence and the differently expressed gene analysis revealed that 18372 transcripts appeared in all samples. During data preprocessing, 1232 low quality transcripts were filtered out and 17140 transcripts were statistically analyzed. As a result, the 1335 transcripts were significantly detected as differentially expressed genes (|fold change|≥2 & Independent t-test raw p-value<0.05). Among them, 653 were up-regulated and 682 were down-regulated by +UVB irradiation treatment (Fig. 21).

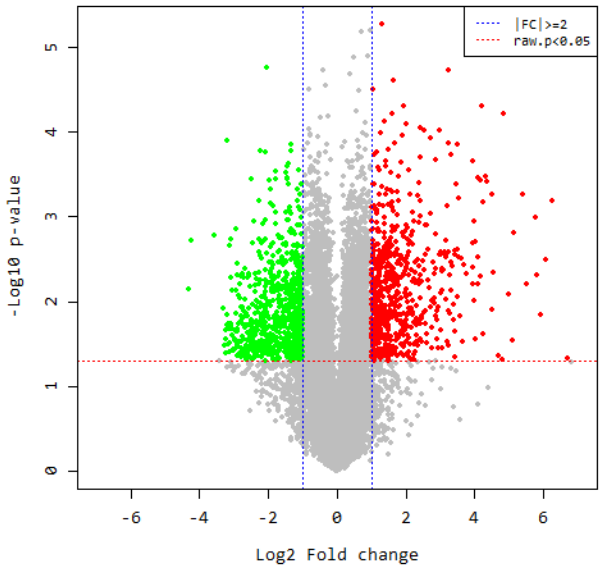

Fig. 21. Volcano plot of differentially expressed genes between "+UVB" and "−UVB" groups identified by RNA-seq. The log10(p-values) were plotted against the log2(FC) in gene expression. Genes upregulated (n = 653) by two-fold or more and with a p-value < 0.05 are depicted as red dots, genes that were downregulated (n = 682) by twofold or more and with a p-value < 0.05 are shown with green dots. All other genes that were not found to be differentially expressed are depicted as grey dots.

In up-regulation, 229 transcripts were uncharacterized. Among identified genes, 25 most up-regulated genes expressed from about 10 to 104 fold changes (Fig. 22). Many proteases and binding proteins, ion-binding, DNA-binding, and lipid-binding genes

were up-regulated (Table 9). Various reactions against UVB stress are expected.

In down-regulation, 224 transcripts were uncharacterized. Among identified genes, the expression levels of 40 most down-regulated genes varied from −20 to −7 fold changes (Fig. 23). While many genes coding functional proteins were noticeable in up-regulation, genes coding structural proteins were significantly confirmed in down-regulated genes. The expressions of myosin heavy chain, muscle-like transcripts were prominently suppressed (Table 10). Among whole down regulation, many cuticle proteins were characteristically down-regulated (Table 11). Furthermore, genes related with epidermis and exoskeletons, like collagen and mucin, were found out in down regulation.

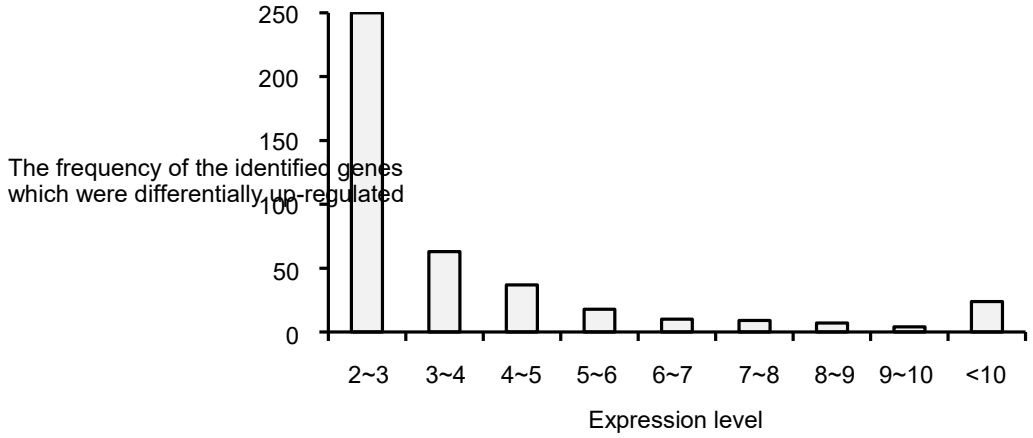

Fig. 22. The identified gene distribution of expression level in significantly up-regulated genes

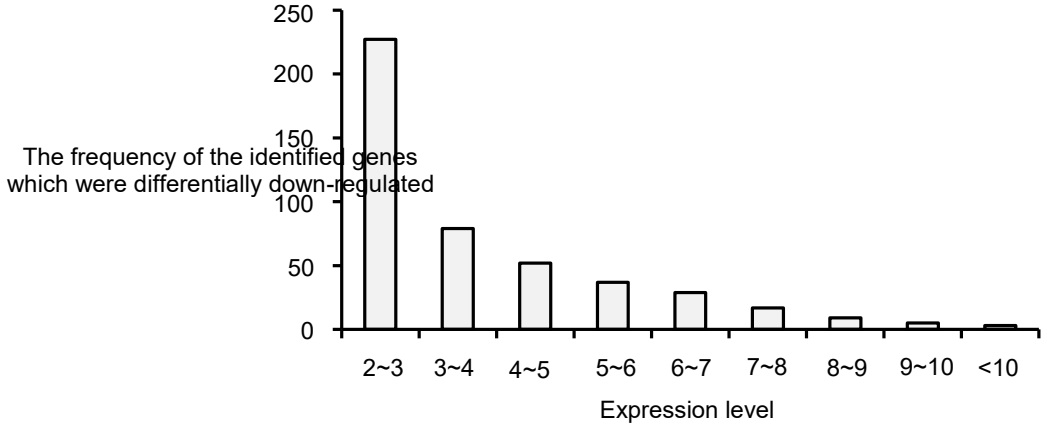

Fig. 23. The identified gene distribution of expression level in significantly down-regulated genes

Table 9. The list of top 30 up-regulated genes induced by UVB irradiation at protochrysalis stage.

Gene ID	Identified Term	FC
107361025	cathepsin B-like	103.91
107371947	wiskott-Aldrich syndrome protein family member 2-like	34.72
107371529	cathepsin B-like	28.09
107368003	keratin-associated protein 6-2-like	23.66
107362104	prisilkin-39-like	22.61
107369352	apolipoprotein D-like	20.45
107372160	cathepsin B-like	19.94
107371946	cell wall integrity and stress response component 1-like	18.04
107371945	forkhead box protein G1-like	17.87
107366560	spidroin-1-like, transcript variant X2	17.20
107359105	agrin-like	17.14
107369350	apolipoprotein D-like	17.02
107369349	apolipoprotein D-like	15.83
107364472	neuropeptide-like protein 33	15.58
107365166	transmembrane protease serine 6-like	15.46
107368043	gamma-glutamyl hydrolase A-like	15.42
107366820	transcription initiation factor TFIID subunit 1-like, transcript variant X1	12.20
107370100	acetylcholinesterase-1-like	11.57
107369827	inactive pancreatic lipase-related protein 1-like	11.56
107365235	DNA-directed RNA polymerase II subunit RPB1-like, transcript variant X1	11.45
107363397	cytochrome P450 307a1-like, transcript variant X1	10.79
107361268	cathepsin L1-like	10.72
107364958	2-amino-3-ketobutyrate coenzyme A ligase, mitochondrial-like	10.36
107363405	UDP-glucose 6-dehydrogenase-like, transcript variant X2	10.05
107367354	acetylcholinesterase-1-like	9.98
107370855	neuroligin-4, X-linked-like	9.38
107359242	alpha-tocopherol transfer protein-like	9.14
107367973	zinc metalloproteinase nas-13-like	9.01
107367758	cathepsin L1-like	8.80
107366282	phytanoyl-CoA dioxygenase domain-containing protein 1 pseudogene	8.31

Table 10. The list of top 30 down-regulated genes induced by UVB irradiation at protochrysalis stage.

Gene ID	Identified Term	FC
107361059	myosin heavy chain, muscle-like, transcript variant X1	−19.73
107361059	myosin heavy chain, muscle-like, transcript variant X4	−19.03
107368509	tyrosine-protein phosphatase 99A-like, transcript variant X1	−11.94
107372112	adult-specific rigid cuticular protein 15.7-like, transcript variant X2	−9.73
107368815	stress protein DDR48-like	−9.40
107371590	bifunctional endo-1,4-beta-xylanase XylA-like, transcript variant X2	−9.37
107371590	bifunctional endo-1,4-beta-xylanase XylA-like, transcript variant X1	−9.12
107369823	elongation of very long chain fatty acids protein AAEL008004-like, transcript variant X2	−9.08
107360423	cuticle protein 14 isoform b-like	−8.96
107361059	myosin heavy chain, muscle-like, transcript variant X5	−8.93
107363734	histidine-rich glycoprotein-like	−8.78
107366510	motile sperm domain-containing protein 2-like	−8.76
107361059	myosin heavy chain, muscle-like, transcript variant X9	−8.64
107360514	GATA zinc finger domain-containing protein 15-like	−8.42
107366745	cuticle protein 14 isoform b-like	−8.39
107368029	acetylcholinesterase-like, transcript variant X2	−8.32
107366963	trinucleotide repeat-containing gene 6B protein-like	−8.21
107363881	nose resistant to fluoxetine protein 6-like	−7.87
107362000	putative uncharacterized protein DDB_G0282133, transcript variant X1	−7.73
107363755	cuticle protein 16.8-like	−7.71
107370316	prostasin-like	−7.65
107359926	collagen alpha-1(V) chain-like	−7.65
107367683	adiponectin receptor protein-like, transcript variant X2	−7.55
107367563	proline-rich extensin-like protein EPR1, transcript variant X2	−7.55
107368456	stress protein DDR48-like	−7.52
107362179	motile sperm domain-containing protein 2-like	−7.48
107363753	perivitellin-2 67 kDa subunit-like	−7.39
107364307	phytoene desaturase-like	−7.36
107366626	mucin-5AC-like	−7.36
107366686	cuticle protein 16.8-like	−7.32

Table 11. The list of cuticle genes which were down-regulated by UVB irradiation at protochrysalis stage.

Gene ID	Identified Term	FC
107372112	adult-specific rigid cuticular protein 15.7-like, transcript variant X2	-9.73
107360423	cuticle protein 14 isoform b-like	-8.96
107366745	cuticle protein 14 isoform b-like	-8.39
107363755	cuticle protein 16.8-like	-7.71
107366686	cuticle protein 16.8-like	-7.32
107370378	cuticle protein 16.8-like	-6.17
107366625	adult-specific rigid cuticular protein 15.5-like	-5.84
107366624	cuticle protein 10.9-like	-3.52
107369924	pupal cuticle protein 36-like	-2.87
107367195	cuticle protein 14 isoform b-like	-2.74

- Discussion

The transcriptome profiling revealed that expressions of genes related with cuticle, chitin, and collagen which are expected to compose the epidermis and exoskeletons during protochrysalis, were significantly suppressed among many variations induced by UVB irradiation at larval stage. It is assumed that the obstruction of metabolism about epidermis and exoskeletons was caused by UVB irradiation. About the life cycles of arthropods, they develop into the next stage with quantitative and functional differentiation (Truman and Riddiford 2002). During these processes, the moulting, in which the old integument was shed and the new one is regenerated, is necessary. The protochrysalis phase-specific death occurred through moult failing, morphological defect, and developmental stop without peeling off and with abnormal contraction of integuments. Therefore, UVB-induced depression of genes about integument tissues might be one of the main causes of these specific lethal effects.

The exoskeleton of arthropods is cuticle, a composite material which is made of the chitin fibers and cuticle proteins. Its physical features have a great variation, depending on its constituents and these cross-linking (Charles 2010). Some previous studies reported the expressions of significant genes of them relating to developmental process.

For instance, in *Drosophila melanogaster*, two chitin synthase genes (*ChS*) were remarkably up-regulated with deposition of epicuticle and pupal lamellate pro-cuticle formation (Gagou et al. 2002). In *Manduca sexta*, *ChS* expression was detected during moulting phase (Zhu et al. 2002). Also in *Bombyx mori* and *Hyphantria cunea*, *ChS*

were expressed during the moulting process (Kim et al. 1998). Additionally, the function analysis was conducted in *M. sexta* (Merzendorfer 2006). The injection of *ChS* double stranded RNA at late larval stage lead to a miscarried metamorphosis and death, with pupae showing abnormal pigmentation and again head deformities. This previous result of RNA interference (RNAi) is corresponded with the verification in this study, in which the lethal effect appeared during pupae and chrysalis stages after treatment on larval stage.

Biosynthesis pathway of chitin was already revealed in insect and it was a multiple reaction, controlled by several enzymes (Trehalase, Hexokinase, Glucose-6-phosphate isomerase, Glutamine:fructose-6-phosphate aminotransferase, Glucosamine-6-phosphate *N*-acetyltransferase, Phosphoacetylglucosamine mutase, UDP-*N*-acetylglucosamine pyrophosphorylase, and Chitin synthase; Kramer and Koga 1986; Cohen 2001; Merzendorfer and Zimoch 2003). Furthermore, these gene expressions were controlled by hormonal process, which upstream was regulated by ecdysteroid and juvenile hormone (Kramer et al. 1993; Zen et al. 1996; Merzendorfer 2011).

In UVB-irradiated *T. urticae*, Glutamine:fructose-6-phosphate aminotransferase gene and UDP-*N*-acetylglucosamine pyrophosphorylase gene were down regulated by −4.17 and −2.42 fold change, respectively. Genes about ecdysteroid were not regulated by UVB irradiation, but gene expression of juvenile hormone acid O-methyltransferase-like was significantly increased by 2.5 fold change. These different expressions suggest that obstruction of chitin synthesis may be one of the causes of UVB-induced phase-specific mortality.

On the other hand, not only regeneration of new chitin but also decomposition of old one is essential during moulting process. The expression of chitin degrading enzyme, chitinase gene (*Cht*) has been also confirmed previously. In *Spodoptera frugiperda*, *Cht* expression was induced during prepupae and pupae stages and chitin existence disappeared during these phases (Bolognesi et al. 2005). In *Panonychus citri*, another *Tetranychidae*, using RNAi method, *Cht* function was verified (Xia et al. 2016). In that study, the phenotype of *P. citri* in which the transcriptome level of the *Cht* was reduced by feeding-based RNAi method was failing of moult and developmental stop at chrysalis stage, corresponding to that of UVB-induced chrysalis phase-specific dead individuals in *T. uritcae* (Fig. 20; Xia et al. 2016). In *T. urticae* genome, more than 20 genes related to chitinase were confirmed. Among them, my results show that 3 probable *Cht* were significantly down-regulated (−4.89, −3.94, and −3.06 fold change) and 2 other related genes were up-regulated (3.84 and 3.49 fold change) by UVB

irradiation. These evidences suggest that factors concerned with degradation of old chitin are essential for growth and development, which may deeply be related with the physiological mechanism of UVB damage.

On expression of cuticle protein which is the other constituent, a high level of transcription occurred during pharate development in association with declining of ecdysteroid titer in honey bee. The transcript was largely regulated during cuticle tanning and sclerotization, suggesting that cuticle protein is essential for morphological differentiation (Soares et al. 2007). In case of *Anopheles gambiae* which devotes over 1% of genome to coding for cuticle proteins, they were grouped into 21 clusters according to expression profiles during each post-ecdysial developmental stage and most of them were up-regulated during moulting phase (Togawa et al. 2008). About silkworm, *Bombyx mori* which employed more than 1.5% of its estimated protein-coding genes to encode cuticle proteins, both the genes coding for critical enzymes for chitin synthesis and the majority of cuticle protein genes were highly expressed at the same stages during development (Liang et al. 2010). *T. urticae* genome also has more than 20 genes coding cuticle proteins. In this verification, 10 genes of them were down-regulated by UVB irradiation (Table11). These facts may suggest that the cuticle protein gene expressions are also closely related with morphological differentiation and moulting in *T. urticae*, and exposure to UVB radiation suppresses these expressions.

Therefore, previous reports and demonstration of UVB effect in this study indicate the possibility that UVB damage causes the obstruction of metabolism of integument tissues and induces the lethal effect during pupal and chrysalis stages at which dynamic physiological change is expected with development and metamorphosis.

Chapter7: General Discussion

This study demonstrated the UVB-induced damage and importance of photoreactivation repair. This would be the first report to prove the UV-induced DNA lesions and importance of physiological repair mechanism on small terrestrial arthropod.

Significant changes of mite survival by UVB and VIS irradiation strongly suggest that solar radiation deeply affects their fitness in terrestrial natural ecosystem. *T. urticae* commonly stays on the lower surface of leaves in nature (Foott et al. 1963). Plant leaves prevent UVB penetration by accumulation of shielding substances such as flavonoids, to protect delicate mesophyll cell from UVB impact (Lavola et al. 1998; Rousseaux et al. 2004; Tegelberg et al. 2004; Izaguirre et al. 2007). Staying on lower side of leaves enables to decrease the harmful effect of UVB (Ohtsuka and Osakabe 2009). Avoidance from UV irradiation was experimentally demonstrated and UVB avoidance was considered the ultimate factor of their staying on lower surface (Sakai and Osakabe 2010). In contrast, this study proved the drastic physiological repair capacity from UVB damage, suggesting some risk to be still remained on the lower leaf surfaces in natural. A phytoseiid mite species, *Typhlodromalus aripo* De Leon, which is the most vulnerable to UVB radiation in comparison to other phytoseiids, was significantly affected by UVB irradiation, in spite of their staying on lower leaf surface, being at the opposite side of UV source across leaf (Onzo et al. 2010). UVB reflections may reach the lower side to some extent, and wind blowing may turn leaves upside down. A variety of solar altitude would also make some fractions of sunlight possible to reach under side. Hence, *T. urticae* may be much more exposable to UVB than that seems to be, and even tiny little UVB fraction has serious impact for their life. It is appropriate to think that they avoid direct UV exposure by behavioral strategy and physiological repair system plays an essential role to survive remaining UVB stress. Terrestrial arthropods are considered to be well protected against UV damage by exoskeletons, coats, and behavior (Paul and Gwynn-Jones 2003). In addition, repair system probably sustains their UV adaptation. In Tetranychidae, there is a difference in species preference of leaf surface to stay on. Citrus red mite, *Panonychus citri*, prefers upper surface whereas *T. urticae* stays on lower side of leaves (Jones and Parrella 1984; Morimoto et al. 2006; Osakabe et al. 2006). *P. citri* is more tolerant to direct exposure to UVB than *T. urticae* (Fukaya. et al. 2013). To live under UV stress, important may be the balance of each dependence on shielding/avoidance behavior/repairing damage to decide the mode of terrestrial life for organisms.

The differences of vulnerabilities and behavioural responses between and within herbivorous and predacious mite groups (Tachi and Osakabe 2012, 2014; Fukaya et al. 2013) suggest that daily and seasonal variation of solar UVR would affect mite community on plants. For example, *T. aripo* hides inside domatia on cassava plants during the day and forages on leaves at night (Onzo et al. 2010), implying that solar UVB radiation is a natural selective force on plant-dwelling mite communities. Moreover, the recent attenuation of ozone layer with increasing UVB radiation is one of the main environmental threats in the future. The result of this study also suggests that increasing of UVB radiation seems to have a great impact on terrestrial small ecosystems.

The lethal effect of UVB which had been shown on the field experiment by Ohtsuka and Osakabe (2009) was confirmed by laboratory experiment in this study; the great harmful impact of UVB on life maintenance of *T. uritcae* was demonstrated again. In this study, UV-induced DNA damages, CPDs and 6-4PPs, were found on UVB-irradiated *T. urticae* larvae. Probably, this is the first verification on terrestrial living organisms, particularly on arthropods, and would be the important evidence that UVB radiation physiologically affects the organisms being adapted for terrestrial environment. In terms of photoreactivation mechanism, VIS-induced decrease of CPD was proved on larvae, suggesting the CPD photolyase function. It suggests the existence and importance of PER mechanism for physiological adaptation to UVB stress. Unexpectedly, the gene expression of CPD photolyase did not increase significantly by UVB and VIS irradiation. Though there are some reports showing this expression on cultured cell and bacteria (Sebastian et al. 1990; Yasuhira and Yasui 1992; Berrocal-Tito et al. 1999), the consistent trend of its induction has never been appeared. This finding is the first in terrestrial living organisms and thus it will make an important step to construct the story of photolyase function. In contrast, the gene expression of XPA, a core factor of NER mechanism, was significantly induced by UVB and VIS irradiation. Not only PER but also NER function may deeply contribute to repairing DNA damage as shown in other organisms (Mitchell et al. 2009; Kienzler et al. 2013). In particular, *T. urticae* does not possess (6-4) photolyase and produced 6-4PPs were not actually repaired by VIS irradiation. 6-4PPs are known for their very cytotoxic effect due to large distortion of DNA (Sinha and Häder 2002). Possible association of NER to decrease such harmfulness was indicated by regulation of XPA gene.

For UVB-irradiated larvae, the phase-specific death occurred at the next developmental stage, protochrysalis. Though the UVB-induced mortality was previously reported in many organisms, such phase-specific severe mortality has never

been reported in metazoan. This new finding is the novel information about physiological mechanism of UVB damage. In addition, as a result of whole transcriptome comparison between protochrysalises which were exposed or non-exposed to UVB at larval stage, the large gene depressions about epidermis and exoskeleton, including cuticle protein genes, were confirmed. In this experiment, I just profiled transcriptome and did not verify the relation of DNA damage and each function analysis. Whereas I recognize the necessity of further detailed verification, it may be that the degradation and regeneration of exoskeleton are essential for development through moulting and UVB disarranges its mechanisms, since protochrysalis phase-specific death occurred through moult failing, morphological defect, and developmental stop without peeling off and with abnormal contraction of integuments. Moreover, some cuticle gene expressions of them were previously validated among each developmental phase, embryo, larvae, nymph, and adult individuals in *T. urticae* (Grbić et al. 2011); higher expression levels of these genes were confirmed in embryo phase. During egg development, embryogenesis, dynamic physiological changes were assumed in relation to larval body formation, as well as chrysalis stages. In addition, it has been already revealed that eggs aged 24–48 h after oviposition is the most vulnerable to UVB radiation for the embryogenesis, which timing consists with the important blastocyst formation (Murata and Osakabe 2014; Dearden et al. 2002). Then, same as protochrysalis phase-specific mortality, obstruction of cuticle exoskeleton formation might induce high UVB vulnerability of eggs.

In *T. urticae* larvae, the survivals of individuals irradiated by UVB at 100% lethal level were fully recovered by VIS irradiation. Thus, the mechanism about epidermis metabolism could also be restored by photoreactivation. On the other hand, VIS irradiation did not induce full recovery on UVB-irradiated eggs. On eggs, the photoreactivation efficiency was depended on the VIS dose and leveled off; the recovery had an upper limit. This limitation is considered to be related to phase-specific mortality, obstruction of cuticle metabolism. According to the time scale of egg development, VIS irradiation might be too late to restore UVB-induced collapse of exoskeletons by photoreactivation. To clarify the complete physiological process about UVB damage and photoreactivation reapir, more detailed time and developmental sequences about transcriptome and function analysis are required.

Studies on the genetic and molecular mechanism of UVB damage and its repair are currently underway. The data presented here would provide the important trigger to clarify the physiological mechanism and ecological significance about UV adaptation in spider mites.

From the view point of pest management, information provided in this study can contribute to UVB application for controlling mites. The reciprocity law in UVB-induced mortality provides the information how mortality is induced by the dose of UVB lamp. Hence, it will be the criterion to set up the time and intensity of UVB irradiation for practical application to control the mites. Conventionally, exposure to UVB for pest management had been recommended to conduct in the day time (Kanto et al. 2014). However, since the high photoreactivation effect was experimentally demonstrated here, night time application of UVB irradiation without solar VIS radiation may be preferable also in agriculture. Moreover, the time lag effect was found in eggs, in which the survival recovery induced by photoreactivation effect was reduced by increasing time lag from UVB irradiation until exposure to VIS light and it disappeared when the time lag was longer than 4h. Therefore, UVB irradiation at night and setting up the irradiation well before 4h to sunrise are recommended to achieve high efficacy. In practice, Tanaka et al. (2016) irradiated strawberry plants with UVB lamp for 3h at night (23:00–2:00 hours), which the time lag between the end of UVB irradiation and sunrise ranged 3–5 h, providing the significant suppression effect of mite population. Contrast to eggs, the time lag effect never appeared in larvae. Therefore, on the developmental stages after larvae, the time lag effect seems not to occur. However, the protochrysalis phase-specific mortality in UVB-irradiated larvae and high UVB vulnerability of teleiochrysalis stage in spite of its relatively large body size showed the proof that UVB lethal effect becomes higher at chrysalis stages. Probably, high mortalities of chrysalis strongly assist the mite suppression effect in application. Furthermore, transcriptome analysis suggested the possibility that UVB-induced obstruction of exoskeleton and epidermal tissue metabolism was one of the main causes of high UVB vulnerability of chrysalis. The cuticle protein genes and the genes related to chitin metabolism which were abnormally expressed by exposure to UVB, are assumed to have the important role in development, moulting, and metamorphosis in arthropods (Gagou et al. 2002; Bolognesi et al. 2005; Merzendorfer 2006; Soares et al. 2007; Liang et al. 2010; Xia et al. 2016). Since the exploitation of pesticides with new action mechanisms are ongoing by many companies and feasibility of utilizing RNAi techniques for pest management is increased gradually, such proteins and genes may potentially become the novel targets for them.

Solar UVR is the essential original energy source, but it has various ecological impacts including serious cause of physiological damage. The studies about such effects have just started and are now gathering great attention. UVB damage and photoreactivation effect presented here can provide the novel perspective on the

evaluation of terrestrial small ecosystem and important clues for improvement of agriculture and environmental conservation. Therefore, UV adaptation in terrestrial organism is the important research topic which further verifications are expected.

SUMMARY

This is the first report demonstrating that the Bunsen–Roscoe reciprocity law is applicable on UVB damage in a terrestrial animal. Mortality caused by UVB was determined by cumulative irradiance regardless of intensity and irradiation time length in *T. urticae*.

Sakai et al. (2012) estimated a LD_{50} value of *T. urticae* eggs by solar UVB radiation as ~50 kJ m^{-2}, which was 86 times the LD_{50} for eggs (0.58 kJ m^{-2}) and twice that for adult females (26.12 kJ m^{-2}) by a UV lamp in laboratory experiments in this study. Sunlight largely consists of visible light much more intense than a fluorescent lamp. Photoreactivation, a phenomenon by PER that exposure to VIS and near-ultraviolet light radiation improves survivals of individuals damaged by UVB, may be a potent factor causing the disagreement between the results in laboratory and outdoor.

In this study, photoreactivation capacity was revealed in *T. urticae*; ~60% and ~100% increasing of hatchability in eggs and survival in larvae, respectively, were induced by exposure to VIS after UVB irradiation. Detail experiments revealed that the photoreactivation efficiency was determined by the cumulative VIS irradiance regardless of intensity and irradiation time length, meaning the reciprocity law. The cumulative VIS irradiance-photoreactivation efficiency curve in *T. urticae* eggs was sigmoid, and the efficiency leveled off at ~200 kJ m^{-2}. This phenomenon might be concerned with the phase-specific vulnerability to UVB in embryogenesis in eggs; an egg at the physiologically changing phase became more vulnerable. Whether UVB damage is repaired by PER up to the UVB vulnerable stage may determine the photoreactivation efficacy.

Wavelengths affected the photoreactivation efficiency. UVA, blue, and green light irradiation raised hatchability significantly but yellow and red light did not, indicating that 350–500 nm light is effective for photoreactivation in *T. urticae*. Generally, many organisms use 350–450 nm of light for photoreactivaiton. Therefore, the results in this study corresponded with the general tendency.

Time lag effect in photoreactivation efficacy was also confirmed. The survival recovery induced by photoreactivation effect reduced by increasing of time lag from UVB irradiation until exposure to VIS light and it disappeared when the time lag became longer than 4h. It was assumed that the decreasing of photoreactivation efficacy in eggs was related to the phase-specific vulnerability of embryogenesis.

One of the most important targets of UVB damage is thought to be DNA. When DNA is exposed to UV radiation, two adjacent pyrimidine bases are linked together by the

high UV energy, producing CPD and 6-4PP. These abnormal structures block transcription and replication of DNA, inducing mutation and death. In *T. urticae*, as in others, CPD and 6-4 PP increased and mortality was induced gradually with increasing UVB dose. This fact suggests that these DNA lesions are one of the main causes of UVB-induced death.

The correspondence between an increase of survivorship and a reduction in CPDs by VIS irradiation indicates that PER of CPDs is a major factor in the photoreactivation of *T. urticae* larvae exposed to UVB irradiation. In contrast, 6-4PP decreased little after VIS irradiation 30 min after UVB irradiation. The difference in the remainings of CPDs and 6-4PPs is compatible with the fact that *T. urticae* possesses CPD photolyase genes, but not (6-4) photolyase genes.

In *T. urticae*, CPD photolyase gene expression was slightly induced by UVB irradiation. VIS irradiation after UVB irradiation did not induce CPD gene expressions. Eventually, CPD photolyase gene expression did not change significantly, even at 100% lethal level of UVB and 100% recovery level of VIS irradiation treatment. Contrary to my expectation, the XPA gene associated with NER was upregulated by UVB irradiation followed by VIS irradiation, rather than the CPD photolyase genes. Thus, there is a possibility that the proximate cause of photoreactivation phenomena is not only due to PER but also to NER induced by UVB and VIS irradiation.

Larvae exposed to UVB radiation looked phenotypically healthy. However, when they developed to the next protochrysalis stage, UVB-induced death highly occurred. Many individuals failed moulting and were trapped in old epidermis, or stop development to eventual shrink. Although the mortalities induced by UVB radiation were reported in many organisms, developmental stage-specific death was never reported for UVB-induced lethal effect in metazoan. In chrysalis stages, the significant physiological changes including DNA replications and gene expressions were expected for development into the next stage. Under these circumstances, I assumed that UVB effects including DNA damages received at larval stage inhibited the replications and transcriptions essential for developmental transformation at protochrysalis stage, inducing the phase-specific lethal effect. As a result of the expression profiling between protochrysalis which was affected or non-affected by UVB irradiation, genes coding structural proteins showed large depression. Particularly, there was a tendency that cuticle protein genes were characteristically suppressed. During the molting processses, it is necessary that the old integument is shed and the new one is regenerated. The protochrysalis phase-specific death occurred through moult failing, morphological defect, and developmental stop without peeling off and with abnormal contraction of

integuments. Therefore, UVB-induced depression of genes about epidermal tissues might be one of the causes of these specific lethal effects.

This study can contribute to elucidate the mechanism of UV damage and its repair for constitutional understanding of UV adaptation. Additionally, because *T. urticae* is an important agricultural pest, this information can contribute to improve the possible physical strategy of pest management using UVB radiation

REFERENCES

Abbott WS (1925) A method of computing the effectiveness of an insecticide. J Econ Entomol **18**: 265–267.

Ahmed MdK, Habibullah-Al-Mamun Md, Hossain MA, Arif M, Parvin E, Akter MS, Khan MS, Islam MdM (2011) Assessing the genotoxic potentials of arsenic in tilapia (*Oreochromis mossambicus*) using alkaline comet assay and micronucleus test. Chemosphere **84**:143–149.

Aoki S (2011) Statistic Analysis Using R, Ohmsha, Tokyo, 320 p.

Baalen CV, O'Donnell R (1972) Action spectra for ultraviolet killing and photoreactivation in the blue-green alga *Agmenellum quadruplicatum*. Photochem Photobiol **15**:269–274.

Ballaré CL, Caldwell MM, Flint SD, Robinson SA, Bornman JF (2011) Effects of solar ultraviolet radiation on terrestrial ecosystems. Patterns, mechanisms, and interactions with climate change. Photochem Photobiol Sci **10**: 226–241.

Bancroft BA, Baker NJ, Blaustein AR (2007) Effects of UVB radiation on marine and freshwater organisms: a synthesis through meta-analysis. Ecol Lett **10**: 332–345.

Barcelo JA, Calkins J (1980) The kinetics of avoidance of simulated solar UV radiation by two arthropods. Biophys J **32**: 921–930.

Barcelo JA (1981) Photoeffects of visible and ultraviolet radiation on the two-spotted spider mite, *Tetranychus urticae*. Photochem Photobiol **33**: 703–706.

Batty DP, Wood RD (2000) Damage recognition in nucleotide excision repair of DNA. Gene **241**:193–204.

Bekkaoui F, Poisson I, Crosby W, Cloney L, Duck P (1996) Cycling probe technology with RNase H attached to an oligonucleotide. Biotechniques **20**:240–248.

Berton TR, Mitchell DL (2012) Quantification of DNA photoproducts in mammalian cell DNA using radioimmunoassay. DNA Repair Protocols vol 920. Springer, New York 177–187.

Berrocal-Tito G, Sametz-Bron L, Eichenberg K, Horwitz BA, Herrera-Estrella A (1999) Rapid blue light regulation of a *Trichoderma harzianum* photolyase gene. J Biol Chem **212**:2760–2766.

Bolognesi R, Yasuyuki A, Muthukrishnan S, Kramer KJ, Terra WR, Ferreira C (2005) Sequence of a cDNA and expression of gene encoding chitin synthase and chitinase in the midgut of *Spodoptera frugiperda*. Insect Biochem Mol Biol **35**: 1249–1259.

Britt AB (1996) DNA damage and repair in plants. Annu Rev Plant Physiol Plant Mol Biol **47**:75–100.

Budden T, Bowen NA (2013) The role of altered nucleotide excision repair and UVB-induced DNA damage in melanomagenesis. Int J Mol Sci **14**:1132–1151.

Caldwell MM, Bornman JF, Ballaré CL, Flint SD and Kulandaivelu G (2007) Terrestrial ecosystems, increased solar ultraviolet radiation, and interactions with other climate change factors. Photochem Photobiol Sci **6**: 252–266.

Charles JP (2010) The regulation of expression of insect cuticle protein genes. Insect Biochem Mol Biol **40**: 205–213.

Chiang T, Rupert CS (1979) Action spectrum for photoreactivation of ultraviolet irradiated marsupial cells in tissue culture. Photochem Photobiol **30**:525–528.

Cohen E (2001) Chitin cynthesis and inhibition: a revisit. Pest Manag Sci **57**: 946–950.

Connelly SJ, Moeller RE, Sanchez G, Mitchell DL (2009) Temperature effects on survival and DNA repair in four freshwater cladoceran *Daphnia* species exposed to UV radiation. Photochem Photobiol **85**: 144–152.

Coohill TP, Sagripanti J-L (2009) Bacterial inactivation by solar ultraviolet radiation compared with sensitivity to 254 nm radiation. Photochem Photobiol **85**: 1043–1052.

Cywinska A, Crump D, Lean D (2000) Influence of UV radiation on four freshwater invertebrates. Photochem Photobiol **72**: 652–659.

Dearden PK, Donly C, Grbić M (2002) Expression of pair-rule gene homologues in a chelicerate: early patterning of two-spotted spider mite *Tetranychus urticae.* Development **129**:5461–5472.

Dworkin M (1958) Endogenous photosensitization in a carotenoidless mutant of *Rhodopseudomonas spheroids*. J Gen Physiol **41**: 1099–1112.

Foggo A, Higgins S, Wargent JJ and Coleman RA (2007) Tri-trophic consequences of UV-B exposure: plants, herbivores and parasitoids. Oecologia **154**: 505–512.

Foott WH (1963) Competition between two species of mites. II. Factors influencing intensity. Can Entomol **95**:45–57.

Fukaya M, Uesugi R, Ohashi H, Sakai Y, Sudo M, Kasai A, Kishimoto H, Osakabe Mh (2013) Tolerance to solar ultraviolet-B radiation in the citrus red mite, an upper surface user of host plant leaves. Photochem Photobiol **89**: 424–431.

Gagou ME, Kapsetaki M, Turberg A, Kafetzopoulos D (2002) Stage-specific expression of the chitin synthase DmeChSA and DmeChSB gene during the onset of Drosophila metamorphosis. Insect Biochem Mol Biol **32**: 141–146.

Gillet LCJ, Schärer OD (2006) Molecular mechanisms of mammalian global genome nucleotide excision repair. Chem Rev **106**:253–276.

Grbić M, Van Leeuwen T, Clark RM, Rombauts S, Rouzé P, Grbić V, Osborne EJ,

Dermauw W, Ngoc PCT, Ortego F, Hernández-Crespo P, Diaz I, Martinez M, Navajas M, Sucena É, Magalhães S, Nagy L, Pace RM, Djuranović S, Smagghe G, Iga M, Christiaens O, Veenstra JA, Ewer J, Villalobos RM, Hutter JL, Hudson SD, Velez M, Yi SV, Zeng J, Pires-daSilva A, Roch F, Cazaux M, Navarro M, Zhurov V, Acevedo G, Bjelica A, Fawcett JA, Bonnet E, Martens C, Baele G, Wissler L, Sanchez-Rodriguez A, Tirry L, Blais C, Demeestere K, Henz SR, Gregory TR, Mathieu J, Verdon L, Farinelli L, Schmutz J, Lindquist E, Feyereisen R, Van de Peer Y (2011) The genome of *Tetranychus urticae* reveals herbivorous pest adaptations. Nature **479**:487–492.

Hanawalt PC (1966) The U.V. sensitivity of bacteria: Its relation to the DNA replication cycle. Photochem Photobiol **5**: 1–12.

Hidema J, Kumagai T, Sutherland BM (2000) UV radiation-sensitive norin 1 rice contains defective cyclobutane pyrimidine dimer photolyase. Plant Cell **12**:1569–1578.

Ikegami Y, Yano S, Takabayashi J, Takafuji A (2000) Function of quiescence of *Tetranychus kanzawai* (Acari: Tetranychidae), as a defense mechanism against rain. Appl Entomol Zool **35**:339–343.

Itabashi M, Higaki S, Fukuda M, Shimomura Y (2010) Detection and quantification of pathogenic bacteria and fungi using real-time polymerase chain reaction by cycling probe in patients with corneal ulcer. Arch Ophthalmol **128**: 535–540.

Izaguirre MM, Mazza CA, Svatoš A, Baldwin IT, Ballaré CL (2007) Solar ultraviolet-B radiation and insect herbivory trigger partially overlapping phenolic responses in *Nicotiana attenuata* and *Nicotiana longiflora*. Ann Bot **99**: 103–109.

Jones VP, Parrella MP (1984) The sublethal effects of selected insecticides on life table parameters of Panonychus citri (Acari: Tetranychidae). The Canadian Entomologist **116**: 1033–1040.

Jurkiewicz BA, Buettner GR (1994) Ultraviolet light-induced free radical formation in skin: an electron paramagnetic resonance study. Photochem Photobiol **59**: 1–4.

Kalthoff K (1975) Compensation for solar UV damage by solar radiation of longer wavelengths. Oecologia (Berl.) **18**:101–110.

Kalthoff K, Urban K, Jäckle H (1978) Photoreactivation of RNA in UV-irradiated insect eggs (*Smittia* sp., Chironomidae, Diptera). II. Evidence for heterogeneous light-dependent repair activities. Photochem Photobiol **27**:317–322.

Kanto T, Matsuura K, Ogawa T, Yamada M, Ishiwata M, Usami T, Amemiya Y (2014) A new UV-B lighting system controls powdery mildew of strawberry. Acta Hort. (ISHS) **1049**: 655–660.

Karentz D (2015) Byond xeroderma pigmentosum: DNA damage and repair in an ecological context. A tribute to James E Cleaver. Photochem Photobiol **91**:460–474.

Kelner A (1949) Effect of visible light on the recovery of *Streptomyces griseus* conidia from ultra-violet irradiation injury. Proc Natl Acad Sci USA **35**: 73–79

Kelner A (1951) Action spectra for photoreactivation of ultraviolet-irradiated *Escherichia coli* and *Streptomyces griseu*s. J Gen Physiol **34**:835–852.

Kienzler A, Bony S, Devaux A (2013) DNA repair activity in fish and interest in ecotoxicology: A review. Aquat Toxicol 134-135, 47–56.

Kim MG, Shin SW, Bae K-S, Kim SC, Park H-Y (1998) Molecular cloning of chitinase cDNAs from the silkworm, *Bombyx mori* and the fall webworm, *Hyphantria cunea*. Insect Biochem Mol Biol **28**: 163–171.

Kouwenberg JHM, Browman HI, Cullen JJ, Davis RF, St-Pierre J-F, Runge JA (1999) Biological weighting of ultraviolet (280–400 nm) induced mortality in marine zooplankton and fish. I. Atlantic cod (*Gadus morhua*) eggs. Mar Biol **134**: 269–284.

Kramer KJ, Koga D (1986) Insect chitin: Physical state, synthesis, degradation and metabolic regulation. Insect Biochem **16**: 851–877.

Kramer KJ, Corpuz L, Choi HK, Muthukrishnan S (1993) Sequence of a cDNA and expression of the gene encoding epidermal and gut chitinases of *Manduca sexta*. Insect Biochem Mol Biol **23**: 691–701.

Lavola A, Julkunen-Tiitto R, Roininen H, Aphalo P (1998) Host-plant preference of an insect herbivore mediated by UV-B and CO_2 in relation to plant secondary metabolites. Biochem Syst Ecol **26**: 1–12.

Li YF, Kim S-T, Sancar A (1993) Evidence for lack of DNA photoreactivating enzyme in humans. Proc Natl Acad Sci USA **90**:4389–4393.

Li S, Paulsson M, Björn LO (2002) Temperature-dependent formation and photorepair of DNA damage induced by UV-B radiation in suspension-cultured tobacco cells. J Photochem Photobiol B Biol **66**:67–72.

Liang J, Zhang L, Xiang Z, He N (2010) Expression profile of cuticular genes of silkworm, *Bombyx mori*. BMC Genom **11**: 173.

Livak KJ, Schmittgen TD (2001) Analysis of relative gene expression data using real-time quantitative PCR and the $2^{-\Delta\Delta CT}$ method. Methods **25**:402–408.

Macfadyen EJ, Williamson CE, Grad G, Lowery M, Jeffrey WH, Mitchell DL (2004) Molecular response to climate change: temperature dependence of UV-induced DNA damage and repair in the freshwater crustacean *Daphnia pulicaria*. Global Change Biol **10**: 408–416.

Malloy KD, Holman MA, Mitchell D, Detrich III HW (1997) Solar UVB-induced DNA

damage and photoenzymatic DNA repair in Antarctic zooplankton. Proc Natl Acad Sci USA **94**:1258–1263.

Martin JA, Wang Z (2011) Next-generation transcriptome assembly. Nat Rev Genet **12**: 671–682.

Masui S, Katai Y, Yamada M, Aoki S, Sakurai T, Osakabe M (2013) Effects of UV-B radiation on the reproduction of *Tetranychus ludeni* and the growth of melon plants. Ann Rept Kansai Pl Prot **55**:37–41 (in Japanese with English summary).

Merzendorfer H, Zimoch L (2003) Chitin metabolism in insects: structure, function and regulation of chitin synthases and chitinases. J Exp Biol **206**: 4393–4412.

Merzendorfer H (2006) Insect chitin synthases: a review. J Comp Physiol B Biochem Syst Environ Physiol **176**: 1–15.

Merzendorfer H (2011) The cellular basis of chitin synthesis in fungi and insects: Common principles and differences. Eur J Cell Biol **90**: 759–769.

Mitani H, Shima A (1995) Induction of cyclobutane pyrimidine dimer photolyase in cultured fish cells by fluorescent light and oxygen stress. Photochem Photobiol **61**:373–377.

Mitani H, Uchida N, Shima A (1996) Induction of cyclobutane pyrimidine dimer photolyase in cultured fish cells by UVA and blue light. Photochem Photobiol **64**:943–948.

Mitchell DL, Nairn RS (1989) The biology of the (6-4) photoproduct. Photochem Photobiol **49**:805–819.

Mitchell DL, Scoggins JT, Morizot DC (1993) DNA repair in the veriable platyfish (*Xiphophorus variatus*) irradiated in vivo with ultraviolet B light. Photochem Photobiol **58**:455–459.

Mitchell DL, Adams-Deutsch T, Olson MH (2009) Dose dependence of DNA repair in rainbow trout (*Oncorhynchus mykiss*) larvae exposed to UV-B radiation. Photochem Photobiol Sci **8**:75–81.

Modrusan Z, Bekkaoui F, Duck P (1998) Spermine-mediated improvement of cycling probe reaction. Mol Cell Probes **12**: 107–116.

Morimoto K, Furuicji H, Yano S, Osakabe Mh (2006) Web-mediated interspecific competition among spider mites. J Econ Entomol **99**: 678–684.

Murata Y, Osakabe Mh (2013) The Bunsen–Roscoe reciprocity law in ultraviolet-B-induced mortality of the two-spotted spider mite *Tetranychus urticae*. J insect physiol **59**:241–247.

Murata Y, Osakabe Mh (2014) Factors affecting photoreactivation in UVB-irradiated herbivorous spider mite (*Tetranychus urticae*). Exp Appl Acarol **63**: 253–265.

Murata Y, Osakabe Mh (2016) Photo-enzymatic repair of UVB-induced DNA damage in the two-spotted spider mite *Tetranychus urticae*. Exp Appl Acarol in press.

Nahon S, Porras VAC, Pruski AM, Charles F (2009) Sensitivity to UV radiation in early life stages of the Mediterranean sea urchin *Sphaerechinus granularis* (Lamarck). Sci Total Environ **407**: 1892–1900.

Niu JZ, Dou W, Ding TB, Yang LH, Shen GM, Wang JJ (2012) Evaluation of suitable reference genes for quantitative RT-PCR during development and abiotic stress in *Panonychus citri* (McGregor) (Acari: Tetranychidae). Mol Biol Rep **39**:5841–5849.

Nozawa H, Yamamoto H, Makita K, Schuch NJ, Pinheiro DK, Carbone S, Mac-Mahon RM, Foppiano AJ (2007) Ground-based observations of solar UV radiation in Japan, Brazil and Chile. Rev Bras Geof **25**: 17–25.

Nozawa H, Yamamoto H, Makita K (2010) Ground-based observations of solar UV radiation. ISATE2010: 4th International Symposium on Advances in Technology Education, 28–30 September 2010, Kagoshima, Japan, pp. 251–253.

Ohtsuka K, Osakabe Mh (2009) Deleterious effects of UV-B radiation on herbivorous spider mites: they can avoid it by remaining on lower leaf surfaces. Environ Entomol **38**: 920–929.

Onzo A, Sabelis MW, Hanna R (2010) Effects of ultraviolet radiation on predatory mites and the role of refuges in plant structures. Environ Entomol **39**: 695–701.

Osakabe Mh, Hongo K, Funayama K, Osumi S (2006) Amensalism via webs causes unidirectional shifts of dominance in spider mite communities. Oecologia **150**: 496–505.

Paul ND, Gwynn-Jones D (2003) Ecological roles of solar UV radiation: towards an integrated approach. Trends Ecol Evol **18**: 48-55.

Peak MJ, Peak JG, Moehring MP, Webs RB (1984) Ultraviolet action spectra for DNA dimer induction, lethality, and mutagenesis in *Escherichia coli* with emphasis on the UVB region. Photochem Photobiol **40**:613–620.

R Core Team (2011) R: A Language and Environment for Statistical Computing, Version 2.14.0. R Foundation for Statistical Computing, Vienna, Austria.

R Core Team (2013). R: A language and Environment for Statistical Computing, Version 3.0.0. R Foundation for Statistical Computing, Vienna, Austria.

R Core Team (2014). R: A language and Environment for Statistical Computing, Version 3.1.0. R Foundation for Statistical Computing, Vienna, Austria.

Rastogi RP, Richa Kumar A, Tyagi MB, Sinha RP (2010) Molecular mechanisms of ultraviolet radiation-induced DNA damage and repair. J Nucleic Acids Article ID 592980 32 p.

Reef R, Dunn S, Levy O, Dove S, Shemesh E, Brickner I, Leggat W, Hoegh-Guldberg O (2009) Photoreactivation is the main repair pathway for UV-induced DNA damage in coral planulae. J Exp Biol **212**:2760–2766.

Rhee J, Kim B, Choi B, Lee J (2012) Expression pattern analysis of DNA repair-related and DNA damage response genes revealed by 55 K oligomicroarray upon UV-B irradiation in the intertidal copepod, *Tigriopus japonicas*. Comp Biochem Phys C **155**:359–368.

Richa Kumar A, Tyagi MB, Sinha RP (2010) Molecular mechanisms of ultraviolet radiation-induced DNA damage and repair. J Nucleic Acids Article ID 592980 32 p.

Riley RL, Kaufman JE (1972) Effect of Relative Humidity on the Inactivation of Airborne *Serratia marcescens* by Ultraviolet Radiation. Appl Environ Microbiol **23**: 1113-1120.

Rousseaux MC, Julkunen-Tiitto R, Searles PS, Scopel AL, Aphalo PJ, Ballaré CL (2004) Solar UV-B radiation affects leaf quality and insect herbivory in the southern beech tree *Nothofagus antarctica*. Oecologia **138**: 505–512.

Rozema J, Björn LO, Bornman JF, Gaberščik A, Häder D-P, Trošt T, Germ M, Klisch M, Gröniger A, Sinha RP, Lebert M, He Y-Y, Buffoni-Hall R, de Bakker NVJ, van de Staaij J, Meijkamp BB (2002) The role of UV-B radiation in aquatic and terrestrial ecosystems—an experimental and functional analysis of the evolution of UV-absorbing compounds. J Photochem Photobiol B: Biol **66**: 2–12.

Rupert CS (1975) Enzymatic photoreactivation: overview. In: Hanawalt PC, Setlow RB (ed) Molecular Mechanisms for Repair of DNA, Part A. Plenum Press, New York, pp 73–87.

Sakai Y, Osakabe Mh (2010) Spectrum-specific damage and solar ultraviolet radiation avoidance in the two-spotted spider mite. Photochem Photobiol **86**: 925–932.

Sakai Y, Sudo M, Osakabe Mh (2012) Seasonal changes in the deleterious effects of solar ultraviolet-B radiation on eggs of the twospotted spider mite, *Tetranychus urticae* (Acari: Tetranychidae). Appl Entomol Zool **47**: 67–73.

Sancar A (1994) Structure and Function of DNA Photolyase. Biochemistry **33**:2–9.

Sancar A (2003) Structure and function of DNA photolyase and cryptochome blue-light photoreceptors. Chem Rev **103**:2203–2237.

Santos CD (2005) Photoreactivation of ultraviolet-B damage in *Tyrophagus putrescentiae* (Acari: Acaridae) and *Tetranychus urticae* (Acari: Tetranychidae). Internat J Acarol **31**: 429–431.

Sebastian J, Kraus B, Sancar GB (1990) Expression of the yeast PHR1 gene is induced by DNA-damaging agents. Mol Cell Biol **10**:4630–4637.

Shiroya T, McElroy DE, Sutherland BM (1984) An action spectrum of photoreactivating enzyme from sea urchin eggs. Photochem Photobiol **40**:749–751.

Sinha RP, Häder DP (2002) UV-induced DNA damage and repair: a review. Photochem Photobiol Sci **1**: 225–236.

Soares MPM, Elias-Neto M, Simões ZLP, Bitondi MMG (2007) A cuticle protein gene in the honeybee: Expression during development and in relation to the ecdysteroid titer. Insect Biochem Mol Biol **37**: 1272–1282.

Speidel D (2015) The role of DNA damage responses in p53 biology. Arch Toxicol **89**:501–517.

Sterck L, Billiau K, Abeel T, Rouzé P, Van de Peer Y (2012) ORCAE: online resource for community annotation of eukaryotes. Nat Methods **9**:1041.

Suzuki T, Watanabe M, Takeda M (2009) UV tolerance in the two-spotted spider mite, *Tetranychus urticae*. J Insect Physiol **55**: 649–654.

Suzuki T, Yoshioka Y, Tsarsitalidou O, Ntalia V, Ohno S, Ohyama K, Kitashima Y, Gotoh T, Takeda M, Koveos DS (2014) An LED-based UV-B irradiation system for tiny organisms: System description and demonstration experiment to determine the hatchability of eggs from four *Tetranychus* spider mite species from Okinawa. J Insect Physiol **62**:1–10.

Tachi F, Osakabe Mh (2012) Vulnerability and behavioral response to ultraviolet radiation in the components of a foliar mite prey-predator system. Naturwissenschaften **99**: 1031–1038.

Tachi F, Osakabe Mh (2014) Spectrum-specific UV egg damage and dispersal responses in the phytoseiid predatory mite *Neoseiulus californicus* (Acari: Phytoseiidae). Environ Entomol **43**:787–794.

Tanaka M, Yase J, Aoki S, Sakurai T, Kanto T, Osakabe Mh (2016) Physical Control of Spider Mites Using Ultraviolet-B With Light Reflection Sheets in Greenhouse Strawberries. J Econ Entomol **109**: 1758–1765.

Tegelberg R, Julkunen-Tiitto R, Aphalo PJ (2004) Red:far-red light ratio and UV-B radiation: their effects on leaf phenolics and growth of silver birch seedlings. Plant Cell Environ **27**: 1005–1013.

Thoma F (1999) Light and dark in chromatin repair: repair of UV-induced DNA lesions by photolyase and nucleotide excision repair. EMBO J **18**:6585–6598.

Todo T, Ryo H, Yamamoto K, Toh H, Inui T, Ayaki H, Nomura T, Ikenaga M (1996) Similarity among the Drosophila (6-4) photolyase, a human photolyase homolog, and the DNA photolyase–blue-light photoreceptor family. Science **272**:109–112.

Togawa T, Dunn WA, Emmons AC, Nagao J, Willis JH (2008) Developmental

expression patterns of cuticular protein genes with the R&R consensus from *Anopheles gambiae*. Insect Biochem Mol Biol **38**: 508–519.

Truman JW, Riddiford LM (2002) Endctine insight into the evolution of metamorphosis in insects. Annu Rev Entomol **47**: 467–500.

Ubara M, Osakabe Mh (2015) Suspension of egg hatching caused by high humidity and submergence in spider mites. Environ Entomol **44**: 1210-1219.

United Nations Environment Programme, Environmental Effects Assessment Panel (2012) Environmental effects of ozone depletion and its interactions with climate change: progress report. Photochem Photobiol Sci **11**: 13–27.

Untergasser A, Nijiveen H, Rao X, Bisseling T, Geurts R, Leunissen JAM (2007) Primer3Plus, an enhanced web interface to Primer3. Nucleic Acids Res **35**:W71–W74.

Weber S (2005) Light-driven enzymatic catalysis of DNA repair: a review of recent biophysical studies on photolyase. Biochim Biophys Acta **1707**: 1–23.

Won E, Han J, Lee Y, Kumar KS, Shin K, Lee S, Park HG, Lee J (2015) In vivo effects of UV radiation on multiple endpoints and expression profiles of DNA repair and heat shock protein (Hsp) genes in the cycloid copepod *Paracyclopina nana*. Aquat Toxicol **165**:1–8.

Wübben DL (2000) UV-induced mortality of zoea I larvae of brown shrimp *Crangon crangon* (Linnaeus, 1758). J Plankton Res **22**: 2095–2104.

Xia WK, Shen XM, Ding TB, Niu JZ, Zhong R, Liao CY, Feng YC, Dou W, Wang JJ (2016) Functional analysis of a chitinase gene during the larval-nymph transition in *Panonychus citri* by RNA interference. Exp Appl Acarol **70**:1–15.

Yasuhira S, Mitani H, Shima A (1991) Enhancement of photorepair of ultraviolet-damage by preillumination with fluorescent light in cultured fish cells. Photochem Photobiol **53**:211–215.

Yasuhira S, Yasui A (1992) Visible light-inducible photolyase gene from the goldfish *Carassius auratus*. J Biol Chem **267**:25644–25647.

Zagarese HE, Feldman M, Williamson CE (1997) UV-B-induced damage and photoreactivation in three species of *Boeckella* (Copepoda, Calanoida). J Plankton Res **19**:357–367.

Zen K-C, Choi HK, Krishnamachary N, Muthukrishnan S (1996) Cloning, expression, and hormonal regulation of an insect β-*N*-acetylglucosaminidase gene. Insect Biochem Mol Biol **26**: 435–444.

Zhu YC, Specht CA, Dittmer NT, Muthukrishnan S, Kanost MR, Kramer KJ (2002) Sequence of a cDNA and expression of the gene coding a putative epidermal chitin synthase of *Manduca sexta*. Insect Biochem Mol Biol **32**: 1497–1506.

ACKNOWLEDGEMENT

I would like to express my deepest appreciation to my supervisor, Dr. Mh. Osakabe for his elaborated guidance, invaluable discussion, and providing me this precious study opportunity. I would like to express my sincere gratitude to Dr. H. Amano and Dr. S. Yano for their valuable advises and useful discussion. I would also like to thank laboratory staff, Ms. T. Nakanishi. She has been greatly tolerant and supportive for my study.

My deepest appreciation also goes to Dr. Y. Manabe and Dr. T. Sugawara for direction about gene expression analysis and providing the real time PCR instrument. I would also like to thank Dr. S-J. Yang, Dr. Y. Yasui, and Dr. A. Joraku who gave me generous support and insightful suggestion about transcriptome analysis. I am also indebt to Mr. N. Nakamura and Dr. C. Tanaka for direction about gene cloning techniques.

Special thanks also to the project members of UVB application for agricultural improvement. They kindly welcomed me into the significant conferences and experiments. Thanks are also extended to professors and students around the world who I met through conferences, workshops, and collaborative project. The communications and time spent with them are irreplaceable for me.

I express my gratitude to Japan Society for the Promotion of Science (JSPS) research fellowship (Grant-in-Aid for JSPS Fellows Nos. 26.2085) for supporting this study.

Finally, I wish to thank all of the members of laboratory of Ecological Information for valuable discussion and kind encouragement.